ORIGINAL RESEARCH

Necrotic Myocardial Cells Release Damage-Associated Molecular Patterns That Provoke Fibroblast Activation In Vitro and Trigger Myocardial Inflammation and Fibrosis In Vivo

Weili Zhang, MD, PhD; Kory J. Lavine, MD, PhD; Slava Epelman, MD, PhD; Sarah A. Evans, PhD; Carla J. Weinheimer, MS; Philip M. Barger, MD; Douglas L. Mann, MD

***Background*—**Tissue injury triggers inflammatory responses that promote tissue fibrosis; however, the mechanisms that couple tissue injury, inflammation, and fibroblast activation are not known. Given that dying cells release proinflammatory "damage-associated molecular patterns" (DAMPs), we asked whether proteins released by necrotic myocardial cells (NMCs) were sufficient to activate fibroblasts in vitro by examining fibroblast activation after stimulation with proteins released by necrotic myocardial tissue, as well as in vivo by injecting proteins released by necrotic myocardial tissue into the hearts of mice and determining the extent of myocardial inflammation and fibrosis at 72 hours.

***Methods and Results*—**The freeze–thaw technique was used to induce myocardial necrosis in freshly excised mouse hearts. Supernatants from NMCs contained multiple DAMPs, including high mobility group box-1 (HMGB1), galectin-3, S100β, S100A8, S100A9, and interleukin-1α. NMCs provoked a significant increase in fibroblast proliferation, α–smooth muscle actin activation, and collagen 1A1 and 3A1 mRNA expression and significantly increased fibroblast motility in a cell-wounding assay in a Toll-like receptor 4 (TLR4)- and receptor for advanced glycation end products–dependent manner. NMC stimulation resulted in a significant 3- to 4-fold activation of Akt and Erk, whereas pretreatment with Akt (A6730) and Erk (U0126) inhibitors decreased NMC-induced fibroblast proliferation dose-dependently. The effects of NMCs on cell proliferation and collagen gene expression were mimicked by several recombinant DAMPs, including HMGB1 and galectin-3. Moreover, immunodepletion of HMGB1 in NMC supernatants abrogated NMC-induced cell proliferation. Finally, injection of NMC supernatants or recombinant HMGB1 into the heart provoked increased myocardial inflammation and fibrosis in wild-type mice but not in TLR4-deficient mice.

***Conclusions*—**These studies constitute the initial demonstration that DAMPs released by NMCs induce fibroblast activation in vitro, as well as myocardial inflammation and fibrosis in vivo, at least in part, through TLR4-dependent signaling. **(*J Am Heart Assoc*. 2015;4:e001993 doi: 10.1161/JAHA.115.001993)**

Key Words: damage-associated molecular patterns • fibroblasts • inflammation • innate immunity • myocardial fibrosis

Myocardial injury that results in the death of cardiac myocytes initiates a characteristic inflammatory response that has a remarkably consistent time course, regardless of the specific cause of cell injury. This inflammatory response can be broadly divided into 3 phases: an initial inflammatory phase, a proliferative phase, and a maturation phase.[1] During the past several decades, a great deal has been learned with respect to the identity of the molecules that are responsible for orchestrating the 3 phases of the inflammatory response in the heart.[1,2] However, what has been lacking is a clear understanding of how this response is initiated in the heart after tissue injury.

Germane to the present discussion, recent studies have shown that when cells die via accidental necrosis, regulated necrosis (necroptosis), and/or secondary necrosis (late apoptosis), the release of their cytosolic contents into the extracellular space initiates a brisk inflammatory response that phenocopies the inflammatory response triggered by pathogenic bacteria and/or viruses.[3,4] Because the inflammatory response that ensues after tissue injury occurs in the

From the Division of Nephrology, Department of Internal Medicine, Shanghai General Hospital, Shanghai Jiaotong University School of Medicine, Shanghai, China (W.Z.); Division of Cardiology, Department of Medicine, Center for Cardiovascular Research, Washington University School of Medicine, St. Louis, MO (K.J.L., S.A.E., C.J.W., P.M.B., D.L.M.); Division of Cardiology, Peter Munk Cardiac Centre, Toronto General Hospital and University Health Network (S.E.) and Faculty of Medicine (S.E.), University of Toronto, Ontario, Canada.

Correspondence to: Douglas L. Mann, MD, Division of Cardiology, 660 S Euclid Ave, Campus Box 8086, St. Louis, MO 63110. E-mail: dmann@dom.wustl.edu

Received March 24, 2015; accepted May 7, 2015.

absence of a known pathogenic infection, it is referred to as "sterile inflammation." Matzinger proposed the danger model of immunity[5] to explain how the innate and adaptive immune systems were activated by noninfectious stimuli. Prior models of the immune system had focused on the concept that the primary function of the immune system was to discriminate self from nonself[6] through recognition of molecular motifs on pathogenic bacteria and/or viruses, which were referred to as pathogen-associated molecular patterns (PAMPs).[4,6] The danger model suggests that damaged or dying cells release endogenous damage-associated molecular patterns (DAMPs), which are capable of eliciting inflammatory responses, analogous to the immune response that is triggered by PAMPs. Matzinger postulated that the innate immune system evolved not only to detect molecules that were nonself (PAMPs) but also to detect a subset of intracellular molecules (DAMPs), which were hidden by the plasma membrane (hidden-self) and not ordinarily found in extracellular fluids in the absence of cell death, damage, or stress.

Pioneering work by Janeway and colleagues demonstrated that mammalian cells possess germline-encoded pattern recognition receptors (PRRs) that are capable of recognizing conserved molecular motifs shared by PAMPs and DAMPs.[7] The PRRs that have been implicated in sensing both PAMPs and DAMPs include the canonical PRRs such as Toll-like receptors (TLRs), nucleotide-binding oligomerization domain–like receptors and retinoic acid–inducible gene I receptors, or atypical PRRs such as the receptor for advanced glycation end products (RAGE).[8] Given the aforementioned associations between cell death, inflammation, and tissue repair, we sought to determine whether proteins released by necrotic myocardial tissue were sufficient to activate innate immune responses in the heart. Here, we show for the first time that necrotic myocardial cells (NMCs) release DAMPs that are sufficient to provoke fibroblast activation in vitro and trigger myocardial inflammation and fibrosis in vivo, at least in part through Toll-like receptor-4 (TLR4) signaling. Remarkably, high mobility group box-1 (HMGB1), a ubiquitous DAMP, is required for fibroblast activation in vitro and is sufficient to provoke myocardial inflammation and fibrosis in vivo.

Methods

Cell Culture

Cardiac fibroblasts

Primary cultures of mouse cardiac fibroblasts were prepared from 12-week-old C57BL/6 background mice as described previously.[9]

NIH/3T3 cells

Murine NIH/3T3 fibroblasts was purchased from the American Type Culture Collection and cultured in growth medium, consisting of DMEM (4.5 g/L glucose) supplemented with 10% fetal bovine serum and 6 mmol/L L-glutamine.

Mouse Lines

The C57BL/6 mice and the TLR4-deficient mice (C57BL/6 background [a gift from Shizuo Akira][10]) were maintained in specific pathogen-free environment and were fed pellet food and water ad libitum. All studies were performed with the approval of the Institutional Animal Care and Use Committee at Washington University School of Medicine. These investigations conform to the *Guide for the Care and Use of Laboratory Animals*, published by the National Institutes of Health.

Preparation of NMCs

Myocardial cell necrosis was induced by using the freeze–thaw technique, with a modification of the method described by Scaffidi et al.[11] Briefly, freshly excised 12-week-old C57BL/6 mouse hearts (5 to 8 hearts/batch) were rinsed in cold phosphate-buffered saline (PBS) to remove red blood cells and then minced into ≈10 pieces in chilled PBS. To induce myocardial cell necrosis in normal myocardium, the tissue slices were suspended in PBS and placed in a conical tube that was subjected to 1 to 5 freeze–thaw cycles (10 minutes in methanol on dry ice [<−80°] and 3 minutes in a water bath at 37°C). In preliminary control experiments, we observed that there was no protein released into the supernatant from myocardial samples that had not been subjected to freeze–thaw cycles. After 1 to 5 freeze–thaw cycles, the NMC suspension was centrifuged at 12 000*g* for 10 minutes to separate the pellet (unlysed cells and nuclear fraction) from the cytoplasm (supernatant), and the protein content of the supernatant was determined by using the BCA assay (Pierce, Thermo Scientific). We also observed that 3 freeze–thaw cycles of myocardial tissue yielded near-maximal protein release into the supernatant in the absence of manual manipulation of the tissue (Figure 1A). Accordingly, we standardized the method for inducing myocardial cell necrosis by using 3 freeze–thaw cycles and pooling the supernatants from 5 to 8 hearts, which were subsequently aliquoted and stored at −70°C. The coefficient of variability for the biological activity of the NMC supernatants, measured in terms of fibroblast proliferation (see later), was ≈6.9% (Figure 1B). To further characterize the NMC supernatants, 2 additional experiments were performed. First, NMC supernatants were heated to 100°C for 10 minutes to thermally

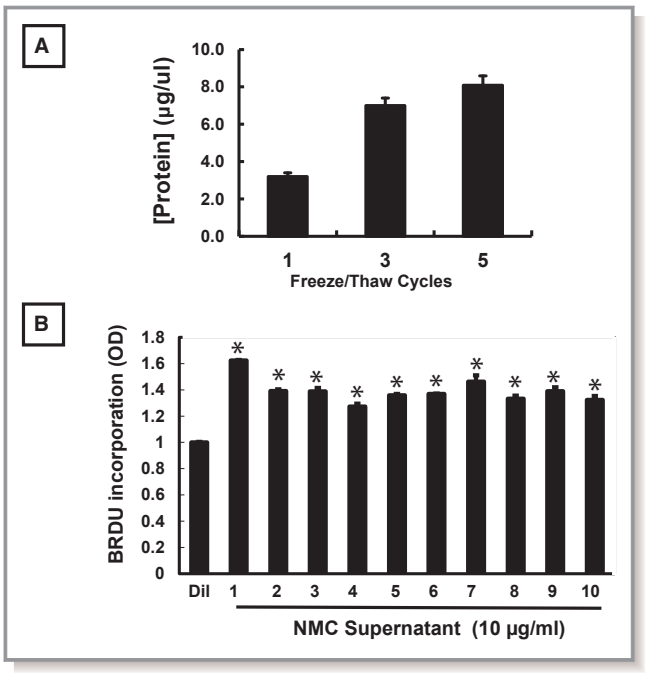

Figure 1. Preparation of cardiac extracts. A, Protein release into supernatant after 1, 3, or 5 sequential freeze–thaw cycles (see text for details) of freshly minced mouse hearts. B, BrdU incorporation in primary cardiac fibroblasts that were treated with 10 µg/mL NMC supernatants obtained from different preparations of cardiac extracts. All experiments were performed in triplicate (*P<0.05 compared with diluent). BrdU indicates bromodeoxyuridine (5-bromo-2′-deoxyuridine); NMC, necrotic myocardial cell; OD, optical density.

denature the proteins in the extracts. Second, the NMC supernatants were treated with DNase (0.5 µg [Sigma-Aldrich]) or RNase (0.05 µg [Sigma-Aldrich]), at concentrations that were sufficient to degrade, respectively, 1 µg plasmid dsDNA or 1 µg total RNA, to remove DNA and/or RNA from the NMC supernatants.

Preparation of Necrotic Liver Cells

Live cell necrosis was induced by the freeze–thaw technique, as described earlier using freshly excised livers obtained from 12-week-old C57BL/6 mice.

Western Blot Analysis

To determine whether NMC supernatants contained DAMPS, Western blot analysis was performed. Briefly, 20-µg cell extracts were separated electrophoretically, and the membranes were incubated with the following antibodies: HMGB1 (1:1000 [Cell Signaling]), galectin-3 (1:200 [Santa Cruz Biotechnology, Inc]), S100β (1:50 [Abcam]), S100A8 (2 µg/mL [R&D systems]), S100A9 (2 µg/mL [R&D systems]), interleukin (IL)-1α (0.5 µg/mL [R&D systems]), LDH (1:200 Santa Cruz [Biotechnology, Inc]), and GAPDH (1:1000 [Santa Cruz Biotechnology, Inc]) overnight at 4°C. The membranes were washed and incubated with the appropriate horseradish peroxidase–conjugated secondary antibodies for 2 hours. Immunoreactive bands were visualized on a Kodak Imagine Station 4000_R Pro by using ECL detection reagent.

Fibroblast Proliferation

The proliferation of primary cardiac fibroblasts and NIH/3T3 fibroblast proliferation was determined by measuring bromodeoxyuridine (5-bromo-2′-deoxyuridine [BrdU]) incorporation as we have described previously,[9] using a commercially available assay (Colorimetric Cell Proliferation ELISA, Roche). The fibroblast cell cultures were treated for 48 hours with PBS, NMC supernatants, or supernatants from necrotic liver cells (NLCs), heat-denatured NMCs and LMCs, NMCs and LMCs treated with DNase (0.5 µg/mL) or RNase (0.05 µg/mL), or 0.1 to 1000 ng/mL recombinant DAMPs (HMGB1 [Sigma-Aldrich], galectin-3 [R&D systems], IL-1α [Cell Signaling], S100β [Sigma-Aldrich], S100A8/A9 [ProSpec-Tany TechnoGene Ltd]) maintained in serum-free DMEM (Sigma-Aldrich), followed by the addition of BrdU for an additional 24 hours. In related experiments, the fibroblast cultures were treated with NMC supernatants for 48 hours in the presence and absence of increasing concentrations of an Akt inhibitor, A6730 (0.1 to 0.5 µmol/L [Sigma-Aldrich]), or increasing concentrations of the ERK inhibitor, U0126 (0.1 to 1.0 µmol/L [Albiochem]), followed by the addition of BrdU for 24 hours.

Fibroblast α–Smooth Muscle Actin Expression

The α–smooth muscle actin (SMA) expression was determined by performing flow cytometric analysis of NIH/3T3 fibroblast cultures that had been stimulated for 48 hours with diluent or NMC supernatants (10 µg/mL), exactly as described earlier.[9] The extent of α-SMA staining in the fibroblast cultures was expressed as the mean fluorescence intensity (MFI).

Fibroblast Collagen Gene Expression

Fibroblast cultures were treated with PBS, mouse NMC supernatants (10 µg/mL), and 0.1 to 1000 ng/mL recombinant DAMPs (HMGB1, galectin-3, IL-1α, S100β, S100A8/A9) for 48 hours. Total RNA was extracted by using TRIzol reagent (Invitrogen). Collagen I (collagen 1A1 and 1A2) and collagen III (collagen 3A1) mRNA levels were quantified by using real-time polymerase chain reaction in cardiac fibroblasts, and levels of gene expression were normalized to 18S ribosomal RNA, as described previously.[9]

Cell-Wounding Assay

A "scratch tip" (cell-wounding) assay was performed to determine whether NMC supernatants stimulated fibroblast migration.[12,13] Briefly, NIH/3T3 fibroblasts were seeded in 6-well plates and cultured in DMEM supplemented with 10% fetal bovine serum until the fibroblasts grew to confluence. The fibroblast cultures were then mechanically disrupted by scratching 2 orthogonal lines (850 to 900 μm in width) in the center of the monolayer with the use of a sterile 200-μL pipette tip. After the cultures were rinsed to remove the disrupted cells, the cell monolayers were refreshed with serum-free DMEM and then stimulated with diluent, NMC supernatants (10 μg/mL), denatured NMC supernatants (10 μg/mL), or basic fibroblast growth factor (bFGF) (25 ng/mL, Sigma-Aldrich), which was used as a positive control. To elucidate the mechanism by which NMC supernatants induced fibroblast migration, the wounded cultures were pretreated for 30 minutes with a neutralizing concentration of a TLR4 antibody (10 μg/mL, rat monoclonal MTS510 to TLR4 [GeneTex]), a murine monoclonal anti-RAGE antibody that did not activate RAGE signaling (500 ng/mL [a generous gift from Dr Ann Marie Schmidt[14]]), or isotype (IgG) control antibodies (10 μg/mL, Sigma-Aldrich) that had no effect on TLR4- or RAGE-dependent signaling. The cultures were then treated with NMC or LMC supernatants, heat-denatured NMC or LMC supernatants, or bFGF for 36 hours. After 36 hours, the cultures were fixed for 30 minutes in 3.7% formaldehyde in PBS and then stained with 0.1% toluidine blue at room temperature for 30 minutes. To standardize the quantification of cell migration in each dish, we enumerated the number of cells that migrated into a region of interest that was defined by the area circumscribed within 2 parallel orthogonal lines (equal to ≈50% of the scratched area). The number of cells migrating into a defined region of interest that was located in the middle of the denuded area (in order to avoid enumerating cells at the edge of the wound) was expressed as total cell number per square millimeter. All measurements were performed by an observer who was blinded to the treatment protocol.

Akt and Mitogen Activated Protein Kinase Signaling

NIH/3T3 fibroblasts were stimulated with NMC supernatants as described above for 0 to 120 minutes, and the cells were harvested and lysed by using RIPA buffer (Sigma). Cell lysates (20 μg of protein) were heat-denatured and fractionated on an Invitrogen NuPAGE 12% gel and then transferred onto pure nitrocellulose membranes. Blots were probed with either anti-Akt, anti-Erk (p44/42), anti–c-Jun, or anti-p38 antibodies to determine the total level of mitogen activated protein kinases (MAPKs) or with phospho-specific antibodies to Akt, Erk (p44/42), c-Jun, or p38 to determine the degree of phosphorylation (ie, activation) of these MAPKs (all reagents from Cell Signaling: Akt rabbit monoclonal antibody [mAb] 4691, phospho-Akt rabbit mAb 4060; p44/42 MAPK (Erk1/2) antibody 9102, phospho-p44/42 MAPK (Erk1/2) rabbit mAb 4370; c-Jun rabbit mAb 9165, phosphor-c-Jun rabbit mAb 2361; p38 MAPK antibody 9212, phospho-p38 MAPK rabbit mAb 4511).

Transcriptional Profiling

To identify potential molecular pathways that were associated with NMC-induced fibroblast activation, we performed a transcriptional profiling on NIH-3T3 fibroblast cultures that were stimulated for 48 hours in serum-free media with either diluent or NMC supernatants (10 μg/mL). Total RNA was extracted from 6 separate culture dishes for each group by using TRIzol reagent (Invitrogen) according to the manufacturer's instructions. RNA was further processed and hybridized to a Mouse Ref-8 Illumina BeadChip by the Genome Technology Access Center at Washington University School of Medicine and scanned with use of the BeadStation system from Illumina, Inc. Quality standards for hybridization, labeling, staining, background signal, and basal level of housekeeping gene expression for each chip were verified, as described.[15] Changes in gene expression were analyzed by using the SAM (Statistical Analysis of Microarray) program and plotted. Expected differentially expressed genes are reported on the *x* axis, whereas observed genes that were differentially expressed are displayed in the *y* axis. A false discovery rate (FDR) <5% was used for the SAM plots. Functional analysis and pathway analysis were performed by using Database for Annotation Visualization and Integrated Discovery (DAVID Bioinformatics Resources 6.7). Lists of genes that were significantly different in the diluent or NMC supernatant-treated fibroblast cultures were analyzed via KEGG (Kyoto Encyclopedia of Genes and Genomes) functional pathway analysis.

Immunodepletion

To identify specific DAMPs that were responsible for the effects of NMC supernatants on fibroblast activation, we performed immunodepletion studies by incubating the NMC supernatants (10 μg/mL) or supernatants containing purified HMGB1 (0.1 μg/mL) with a murine monoclonal HMGB1 2g7 antibody (10 μg/mL, a generous gift from Drs Kevin J. Tracey and Huan Yang[16]) or isotype (IgG2b) control antibodies (10 μg/mL, Sigma-Aldrich) for 30 minutes and then centrifuging the samples at 12 000 g for 10 minutes. After centrifugation, the supernatants were aspirated and used to

stimulate the fibroblast cultures, exactly as described here earlier.

Effects of NMCs In Vivo

To determine whether NMC supernatants would provoke myocardial fibrosis in vivo, we injected NMC supernatants from syngeneic mice into the left ventricular (LV) apex of wild-type C57/Bl6 mouse hearts. Briefly, 12-week-old C57BL/6 background mice were anesthetized with Ket/Xyl (100 mg/10 mg intraperitoneal) and ventilated with use of a Harvard respirator. A left thoracotomy was performed to visualize the anterior wall of the LV. NMC supernatants were injected into the LV apex of the heart by using a 10-μL Hamilton microliter syringe (Microliter TM 701; Hamilton Company). Care was taken to ensure that every injection occurred in the same 2×2-mm space between the left side of the left anterior descending coronary artery, right side of the septal wall, and apex of the LV anterior wall. After the injection of the extracts, the chest was closed, the skin was sutured, and mice were allowed to recover on a warmer until being returned to their cages. In the initial studies, 3 experimental groups of mice were studied: injection of saline (10 μL saline), injection of denatured NMC supernatants (50 μg protein in 10 μL saline), and injection of NMC supernatants (50 μg protein in 10 μL saline). Mice that underwent a thoracotomy and had a visual inspection of the heart, but no direct myocardial injections, were used as the appropriate sham-operated controls (n=5 or 6). In additional experiments using the same protocol, we injected recombinant HMGB1 (200 ng/10 μL, eBioscience) and denatured HMGB1into wild-type C57/Bl6 mouse hearts or hearts of TLR4 knock-out mice (C57/Bl6 background). At 72 hours after surgical recovery, the mice were killed, the hearts were harvested, and paraffin sections were made. Slides were stained with hematoxylin and eosin and picrosirius red acid, as described previously.[9] The degree of myocardial inflammation and myocardial fibrosis were quantified by computer-assisted densitometric analysis of the percentage LV apical myocardium with leukocytic infiltration (×50) or picrosirius red staining (×100).

Statistical Analysis

All results are expressed as mean±SEM values. Data were assessed with the use of commercially available statistical software (SigmaStat 3.1; Systat Software Inc). A Student *t* test was used to evaluate differences in mean fluorescence intensity, α-SMA expression, and collagen mRNA expression between diluent and DAMP-treated fibroblast cultures. One-way ANOVA was used to analyze mean differences in BrdU incorporation, cell migration, Akt and MAPK activation, percent myocardial area with inflammation or fibrosis, and 2-way ANOVA was used to analyze differences and cell migration between diluent and DAMP-treated fibroblast cultures, as well as cell proliferation in the presence and absence of A6730 and U0126 and of HGMB1 and anti-HMG1 antibodies. Where appropriate, post-hoc analysis testing was performed, by using the Holm–Šídák approach for multiple-comparison testing. A value of $P<0.05$ was considered statistically significant.

Results

Characterization of NMC Supernatants

To determine whether NMC supernatants contained DAMPs, we performed Western blot analysis. As shown in Figure 2A, NMC supernatants contained multiple DAMPs, including HGMB1, galectin-3, S100β, S100A8, S100A9, and IL-1α. Noting that release of DAMPs has been associated with renal and liver fibrosis,[17] we asked whether NMC supernatants were sufficient to provoke fibroblast activation, which was defined as (1) increased fibroblast proliferation (BrdU incorporation), (2) percentage of fibroblasts with α-SMA staining, and (3) fibroblast production of extracellular matrix components (COL1A1, COL1A2, and COL3A1 mRNA).[18]

Fibroblast proliferation

Treatment with NMC supernatants for 72 hours provoked a significant ($P=0.012$) concentration-dependent increase in cardiac fibroblast proliferation (Figure 2B). The effects of the NMC supernatants on fibroblast proliferation were abolished after heat denaturation, whereas treatment of the extracts with concentrations of RNase and DNase that were sufficient to degrade RNA (1.0 μg) and DNA (1.0 μg) (Figure 2C) had no significant ($P=0.69$ and 0.47, respectively) effect on cardiac extract-induced fibroblast proliferation (Figure 2B). Figure 2D shows that similar overall results were observed when NIH/3T3 fibroblasts were treated with NMC supernatants. Remarkably, supernatants from NLCs provoked a significant dose-dependent increase in NIH/3T3 fibroblast proliferation (Figure 3), suggesting that the proliferative effects were not unique to myocardial proteins. Given that the effects of the NMC supernatants were similar in cardiac fibroblasts and NIH/3T3 fibroblasts, we performed all subsequent experiments in NIH/3T3 fibroblasts.

α-SMA expression

As shown by the representative flow cytometric analysis illustrated in Figure 4A and group data shown in Figure 4B, the mean fluorescence intensity for α-SMA staining was ≈1.27-fold greater ($P=0.003$) in fibroblasts treated with NMC supernatants compared with diluent stimulated fibroblasts.

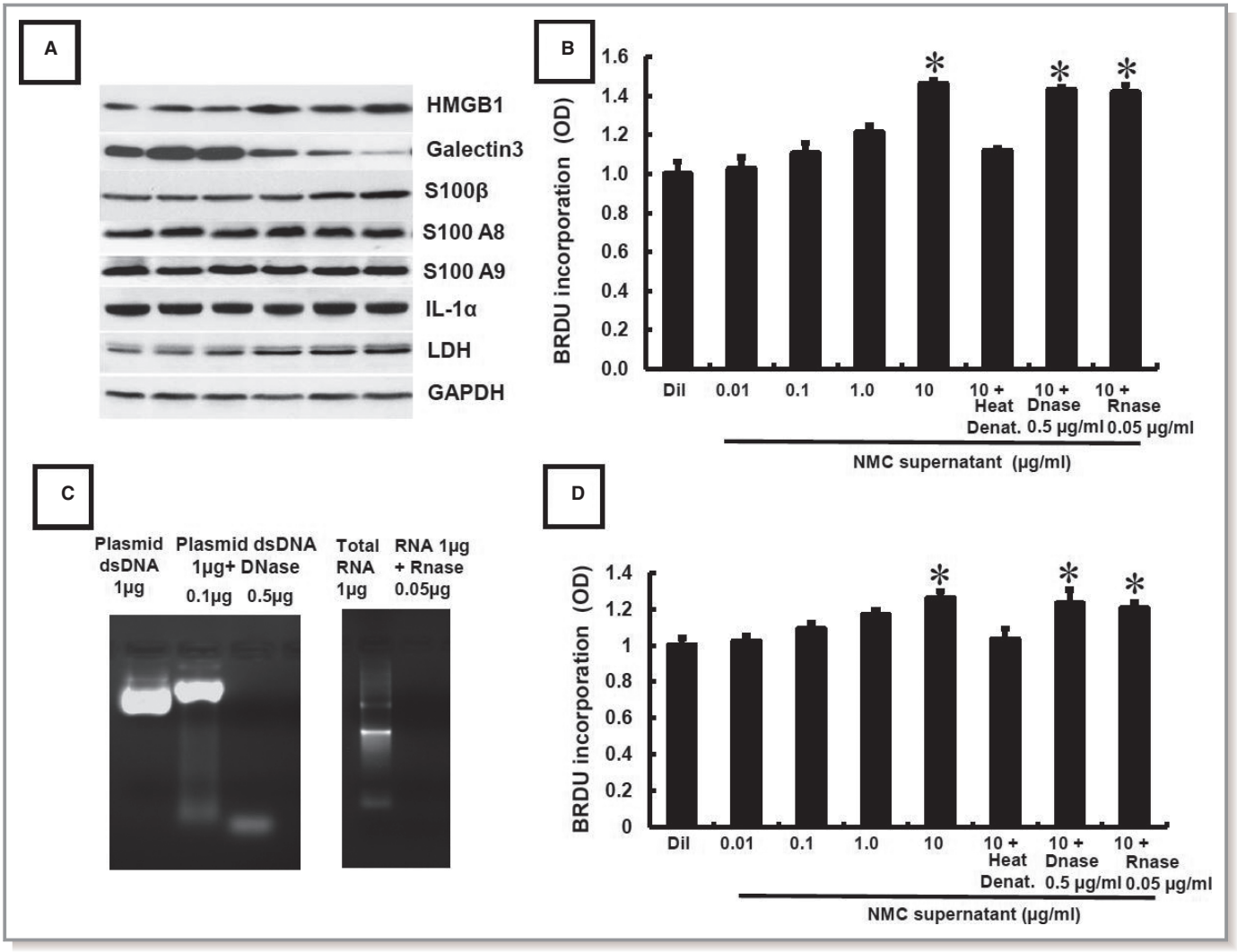

Figure 2. Effect of NMC supernatants on fibroblast proliferation. A, Representative Western blot analyses of NMC supernatants for known DAMPs, including HGMB1, galectin3, S100β, S100A8, S100A9, and IL-1α. B, Effect of diluent (PBS), NMCs, denatured NMCs, and RNase- and DNase-treated NMC supernatants on BrdU incorporation in mouse cardiac fibroblasts (n=6 wells/experimental group from 3 independent experiments). C, Agarose gel of dsDNA (1 μg) and RNA (1 μg) that were treated, respectively, for 30 minutes at 37°C with 0.5 μg/mL DNase and 0.05 μg/mL RNase. D, Effect of diluent (PBS), NMCs, denatured NMCs, and RNase- and DNase-treated NMC supernatants on BrdU incorporation in NIH/3T3 fibroblast proliferation (n=6 wells/experimental group from 3 independent experiments) (*P<0.05 compared with diluent-treated controls). BrdU indicates bromodeoxyuridine (5-bromo-2′-deoxyuridine); DAMP, damage associated molecular pattern; HMGB1, high mobility group box-1; IL, interleukin; LDH, lactate dehydrogenase; NMC, necrotic myocardial cell; OD, optical density; PBS, phosphate-buffered saline.

Collagen gene expression

Figure 4C shows that stimulation with NMC supernatants provoked significant increases in collagen 1A1 (P=0.008) and 3A1 (P=0.007) mRNA levels but had no significant effect (P=0.10) on collagen 1A2 mRNA levels. Viewed together, these observations suggest that NMC supernatants containing DAMPs are sufficient to provoke an activated fibroblast phenotype.

Effect of Recombinant DAMPs on Fibroblast Activation

Given that these studies demonstrated that NMC supernatants contain multiple DAMPs, we next asked whether individual recombinant DAMPs elicited increased fibroblast proliferation and increased collagen gene expression.

Fibroblast proliferation

Figure 5 shows that treatment with HMGB1, galectin-3, and S100A8/A9 significantly (P=0.011, 0.03, and 0.001, respectively) increased fibroblast proliferation in a concentration-dependent manner compared with diluent. However, treatment with IL-1α or S100β had no significant (P=0.34 and 0.43, respectively) effect on fibroblast proliferation. To determine whether individual recombinant DAMPs were synergistic with respect to fibroblast proliferation, we treated fibroblast cultures with subthreshold concentrations of individual DAMPs

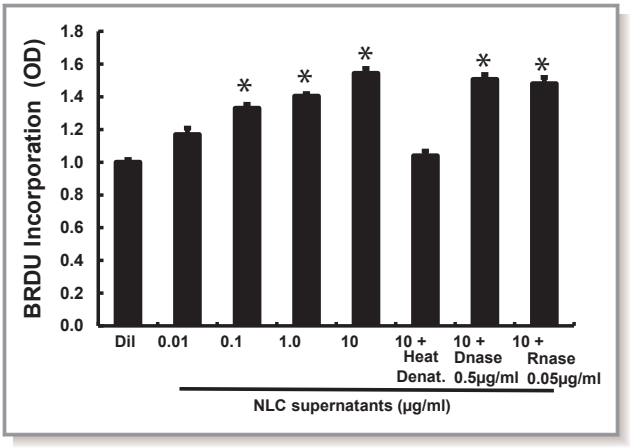

Figure 3. Effect of necrotic liver cells (NLCs) on BrdU incorporation in NIH/3T3 fibroblasts. Fibroblasts cultures were stimulated for 36 hours with diluent (PBS), NLC supernatants (10 μg/mL), D-NLC supernatants (10 μg/mL), NLC supernatants (10 μg/mL) treated with 0.5 μg/mL DNase, and NLC supernatants (10 μg/mL) treated with 0.05 μg/mL RNase (n=6 dishes from 3 separate experiments) (*P<0.05 compared with diluent). BrdU indicates bromodeoxyuridine (5-bromo-2′-deoxyuridine); D-NLC, denatured necrotic liver cell; OD, optical density; PBS, phosphate-buffered saline.

that were not sufficient to increase cell proliferation. As shown in Figure 6, treatment with subthreshold combinations of DAMPs (1 ng/mL HMGB1, 100 ng/mL galectin-3, and 5 ng/mL S100A8 and 5 ng/mL S100A9) significantly (P=0.009) increased fibroblast proliferation ≈1.3-fold compared with diluent-treated controls. Importantly, the fold-change in fibroblast proliferation for 10 μg/mL of NMC supernatants was not significantly (P=0.11) different than the fold-change observed with subthreshold concentrations of multiple DAMPs. These data suggest that low concentrations of individual DAMPs have synergistic effects with respect to fibroblast proliferation.

Collagen gene expression

Treatment with recombinant HMGB1 (1000 ng/mL) and galectin-3 (1000 ng/mL) significantly increased collagen1A1 (P=0.01 and 0.02, respectively) and 3A1 (P=0.02 for both) mRNA expression but had no significant effect (P=0.81 and 0.06, respectively) on collagen 1A2 mRNA levels (Figure 7). In contrast, IL-1α (1000 ng/mL), and S100A8/A9 (500 ng/mL/500 ng/mL) and S100β (1000 ng/mL) had no effect on collagen gene expression in cultured fibroblasts.

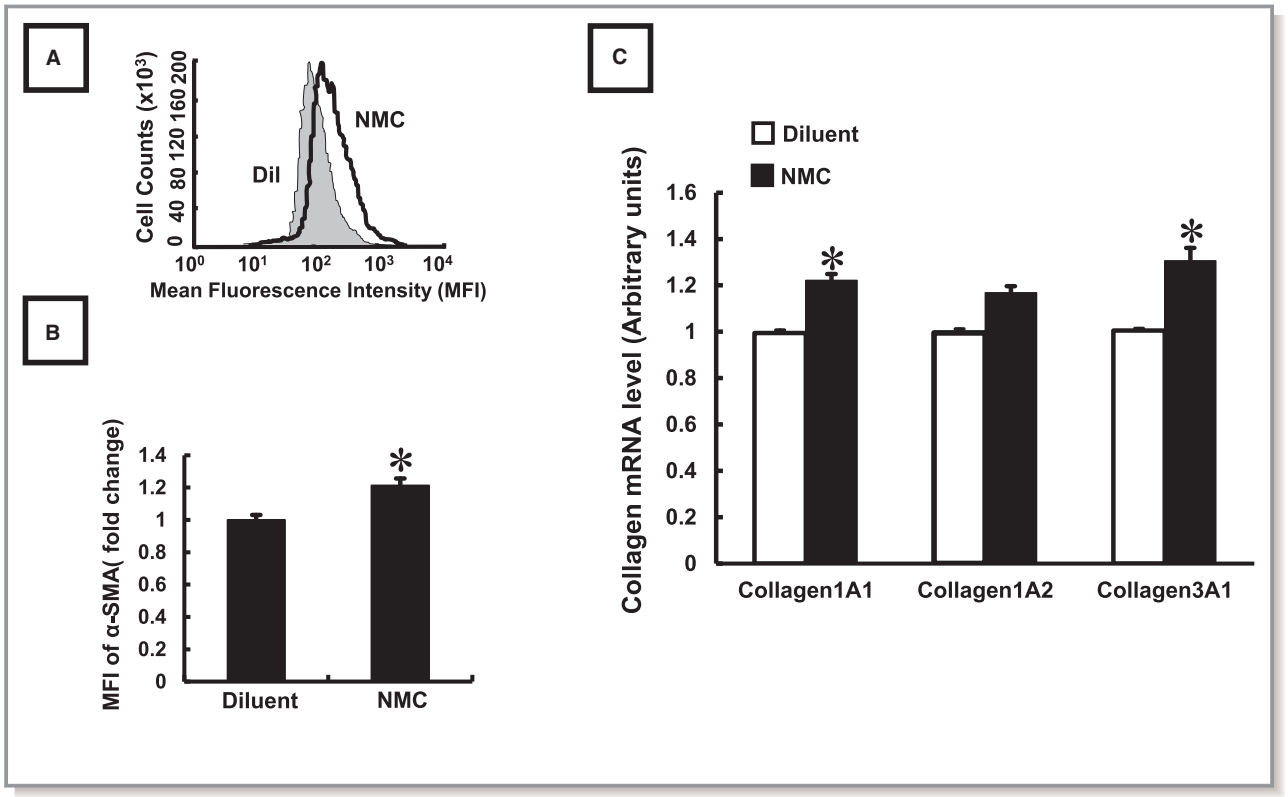

Figure 4. Effect of NMCs on the expression of α-SMA and collagen mRNA levels in NIH/3T3 fibroblasts. A, Representative flow cytometry analysis for α-SMA staining in NIH/3T3 fibroblasts. B, Group data of MFI for α-SMA staining in diluent (PBS)– and NMC (10 μg/mL)–stimulated cardiac fibroblasts. All experiments were performed in triplicate. C, Collagen 1A1, 1A2, and 3A1 mRNA levels in fibroblasts stimulated with diluent or NMC supernatants (10 μg/mL). All experiments were performed in triplicate (*P<0.05 compared with diluent). MFI indicates mean fluorescence intensity; NMC, necrotic myocardial cell; PBS, phosphate-buffered saline; α-SMA, α–smooth muscle actin.

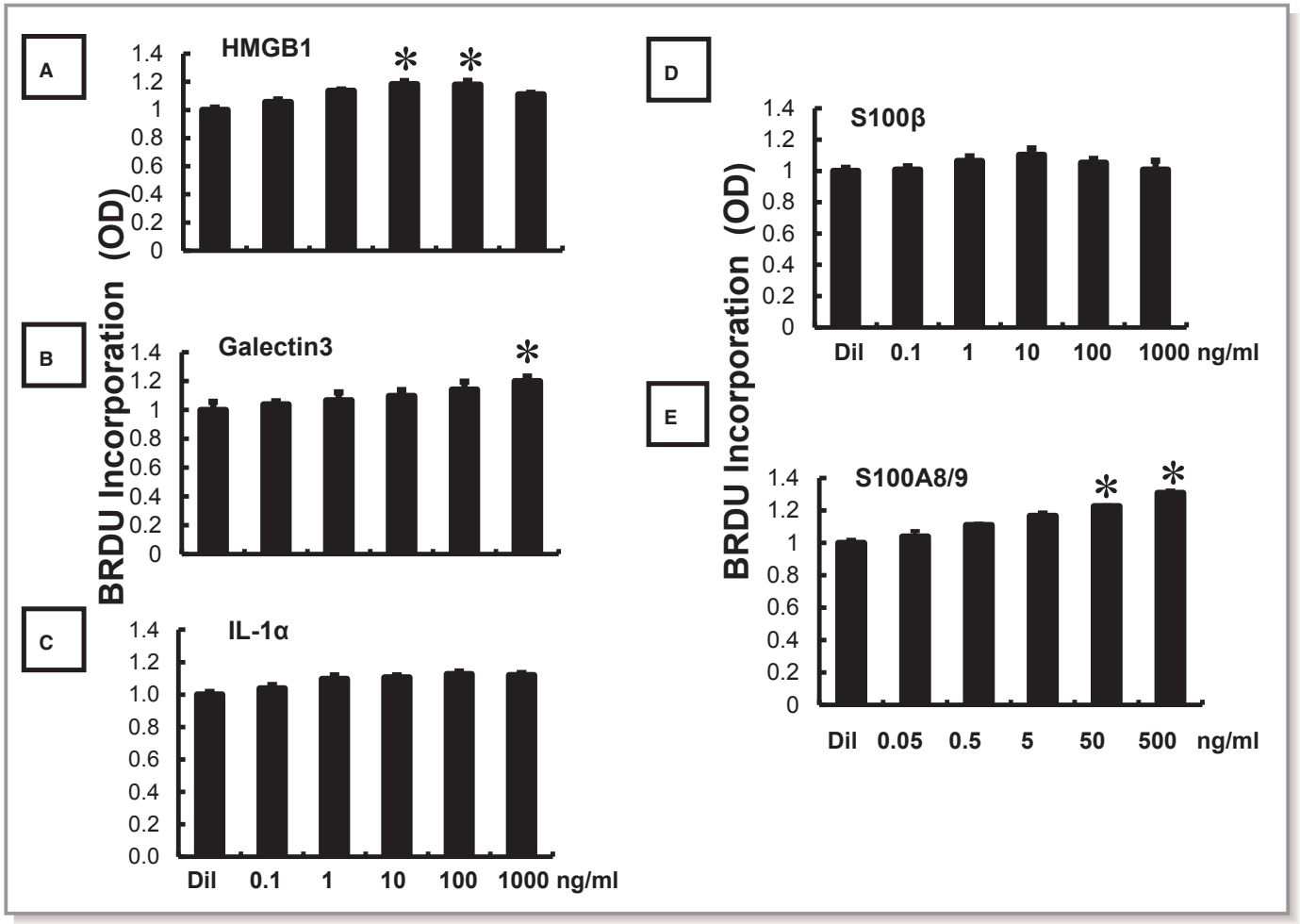

Figure 5. Effects of recombinant DAMPs on BrdU incorporation. NIH/3T3 fibroblast cultures were stimulated for 72 hours with 0.1 ng/mL to 1000 ng/mL of (A) HMGB1, (B) galectin-3, (C) IL-1α, (D) S100β, or (E) a combination of equal concentrations of S100A8 (0.05 to 500 ng/mL) and S100A9 (0.05 to 500 ng/mL). All experiments were performed in triplicate (*P<0.05 compared with diluent). BrdU indicates bromodeoxyuridine (5-bromo-2′-deoxyuridine); DAMP, damage-associated molecular pattern; HMGB1, high mobility group box-1; IL, interleukin; OD, optical density.

Effect of NMCs on Fibroblast Migration

Previous studies have shown that DAMPs can induce cell migration in monocytes, vascular smooth muscle cells, and fibroblasts through TLR4- and RAGE-dependent signaling.[12,13,19–21] To determine whether NMC supernatants stimulated increased fibroblast migration, we performed a cell migration assay by using the "scratch tip" (wound-healing) method.[12,13] Figure 8A shows representative phase-contrast micrographs of confluent fibroblast cell monolayers that were disrupted by scratching 2 orthogonal lines in the monolayer. As shown by the representative photographs in Figure 8A, and summarized in the group data in Figure 8B, both bFGF (P=0.001) and NMC (P=0.001) supernatants provoked increased cell migration compared with diluent. Importantly, the degree of cell migration observed with heat denatured NMCs was not significantly (P=0.21) different from that of diluent-treated cells. Similar effects were observed with respect to cell migration when the fibroblasts were stimulated with supernatants from necrotic liver cells (Figure 9).

To determine whether the effects of NMC supernatants on fibroblast migration were sensitive to inhibition of TLR4 and/or the RAGE signaling pathways, we pretreated the fibroblast cultures with neutralizing TLR4 and RAGE antibodies before stimulating the fibroblasts with NMC supernatants. The salient finding shown in Figure 8C is that cell migration was significantly diminished in the fibroblast cultures treated with neutralizing TLR4 (P=0.01) and RAGE antibodies (P=0.02) compared with NMC-treated cultures with identical concentrations of isotype (IgG) control antibodies that lacked specificity for the TLR4 or RAGE receptors. Importantly, fibroblast migration was completely abrogated by pretreating the cultures with a combination of TLR4 and RAGE antibodies compared with control (P=0.71 compared with diluent). Given

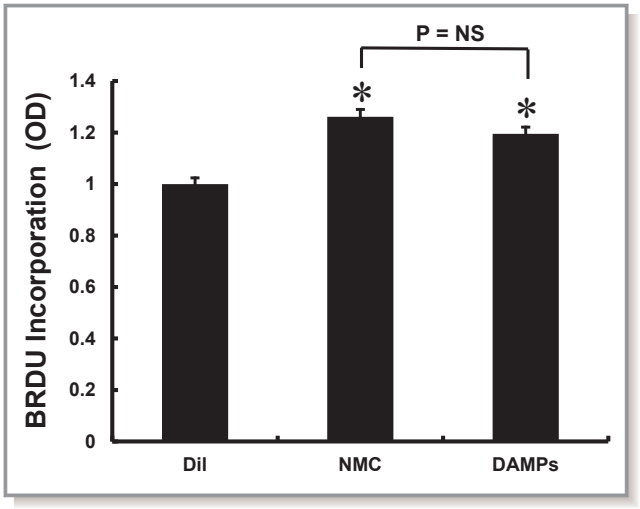

Figure 6. Synergistic effects of subthreshold concentrations of recombinant DAMPs on BrdU incorporation in NIH/3T3 fibroblasts. Fibroblast cultures were treated for 72 hours with diluent, (NMC) supernatants (10 μg/mL), and subthreshold concentrations of DAMPs that were not sufficient to provoke increased BrdU incorporation individually, including HMGB1 (1 ng/mL), galectin-3 (100 ng/mL), and S100A8/A9 (5+5 ng/mL). All experiments were performed in triplicate (*P<0.05 compared with diluent). BrdU indicates bromodeoxyuridine (5-bromo-2′-deoxyuridine); DAMP, damage-associated molecular pattern; HMGB1, high mobility group box-1; NMC, necrotic myocardial cell; OD, optical density.

these findings with respect to cell migration, we also sought to determine whether fibroblast proliferation was sensitive to inhibition of TLR4 and/or RAGE signaling. Figure 8D demonstrates that treatment with neutralizing antibodies to TLR4 and RAGE significantly (P<0.001 and P=0.015, respectively) attenuated cardiac extract-induced fibroblast cell proliferation and was completely abolished by treatment with both TLR4 and RAGE antibodies (P=0.60 compared with diluent). In contrast, isotype (IgG) control antibodies had no significant (P=0.86) effect on cell proliferation. Viewed together, these data suggest that the NMC supernatants stimulate increased fibroblast migration and proliferation through TLR4- and RAGE-dependent signaling pathways. Importantly, liver extracts also provoked a similar increased fold-change in fibroblast cell migration (Figure 9), suggesting that the effects of cardiac proteins on fibroblast proliferation were not unique to the myocardium.

Mechanism of NMC-Induced Fibroblast Proliferation

These studies suggested that NMC supernatants activate fibroblasts through TLR4- and RAGE-dependent signaling pathways. Recognizing that TLR4 and RAGE receptors both signal through Akt- and MAPK-dependent signaling pathways,[12,19] we examined Akt and MAPK activation in NMC-stimulated fibroblast cultures. As shown in Figure 10A through 10D, NMC supernatants triggered a significant time-dependent 3- to 4-fold activation of Akt (P=0.001), Erk (P=0.01), and c-Jun activation (P=0.01) and had no significant (P=0.38) effect on p38 phosphorylation. To determine the role of Akt and Erk signaling pathways in terms of fibroblast activation, we pretreated the fibroblast cultures with A6730 to inhibit Akt signaling, as well as U0126 to inhibit Erk signaling. The important finding shown by Figure 10E and 10F, respectively, is that pretreatment with A6730 and U0126 significantly (P=0.005 and 0.008, respectively) attenuated cardiac extract-induced cell proliferation in a dose-dependent manner. Importantly, the concentrations of A6730 and U0126 that were used decreased NMC-induced Akt and Erk phosphorylation (Figure 11) but did not affect baseline levels of fibroblast cell proliferation (Figure 10E and 10F).

Transcriptional Profiling

The results of the transcriptional profiling studies in fibroblast cultures stimulated with diluent and NMC supernatants are summarized in Figure 12. The SAM plot shown in Figure 12A reveals that stimulation of fibroblast cultures for 48 hours resulted in the differential expression of 996 genes, including 536 genes that were significantly upregulated and 460 genes that were significantly downregulated compared with diluent treatment. An gene ontological analysis of differentially expressed genes indicated that the genes that were significantly increased in the fibroblasts stimulated by NMC supernatants were significantly enriched for cellular functions related to tissue injury and repair, including regulation of cell death, regulation of growth, cell proliferation, response to wounding, cell migration/shape and vasculature development, and angiogenesis (Figure 12B). The specific changes in gene expression for the regulation of cell growth and response to cell-wounding gene ontological pathways are summarized in Figure 12C and 12D.

Effects of NMCs In Vivo

To determine whether NMC supernatants were sufficient to provoke myocardial inflammation and/or myocardial fibrosis in vivo, we injected syngeneic NMC supernatants into the LV apex of wild-type mouse hearts. Figure 13A displays representative histological myocardial sections from hearts subjected to sham operation or hearts that were injected with saline, NMC supernatants, or denatured NMC supernatants, whereas Figure 13B summarizes the group data for these experiments. Both injection of saline and denatured NMC supernatants provoked a mild inflammatory response that was significantly (P=0.003 and 0.004, respectively) greater

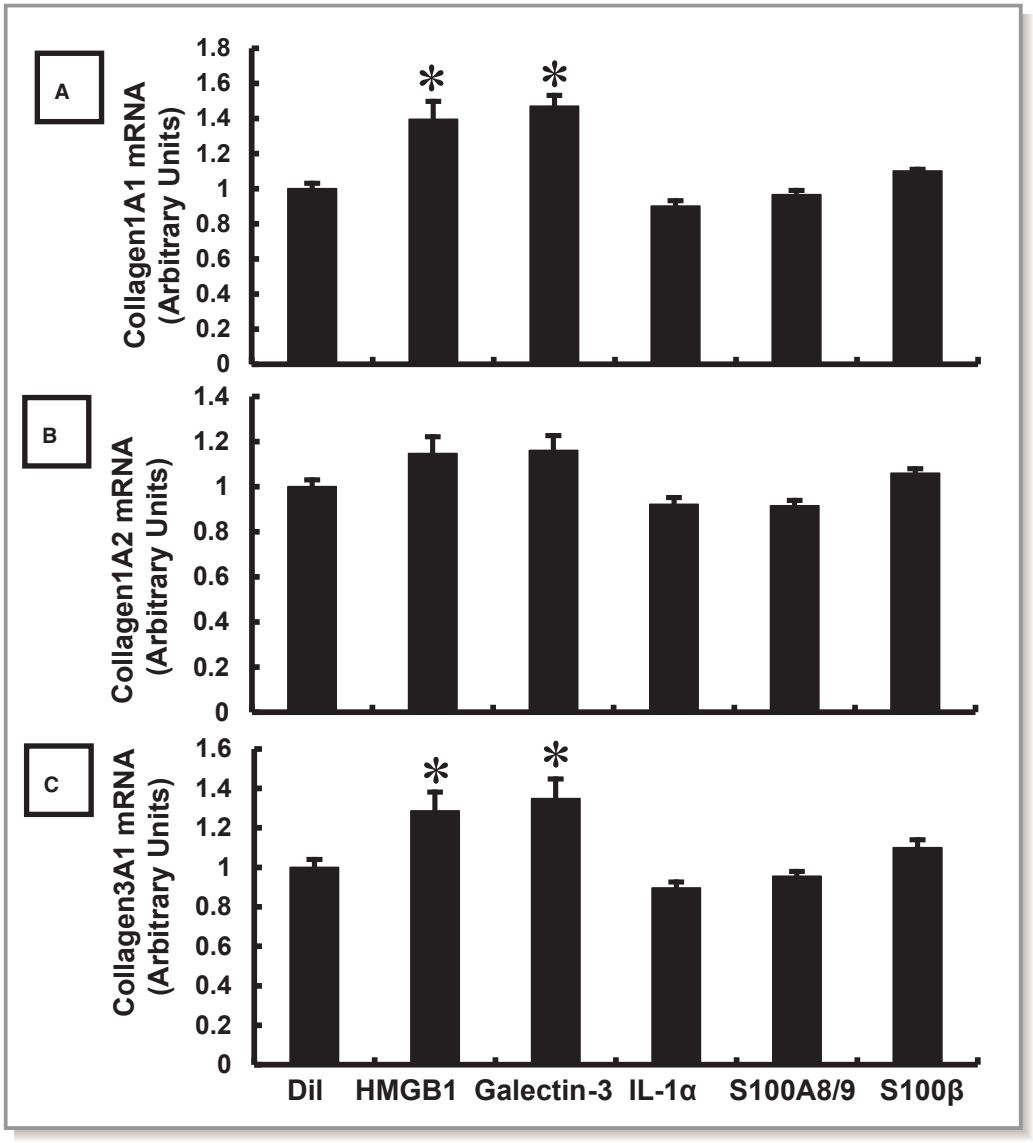

Figure 7. Effect of recombinant DAMPs on collagen mRNA expression. NIH/3T3 fibroblast cultures were stimulated for 48 hours with PBS, 1000 ng/mL HMGB1, 1000 ng/mL galectin-3, 1000 ng/mL IL-1α, 500 ng/mL/500 ng/mL of S100A8/A9, and 1000 ng/mL S100β, and collagen 1A1 (A), 1A2 (B), and 3A1 (C) mRNA levels were determined by real-time PCR. All experiments were performed in triplicate (*$P<0.05$ compared with diluent). DAMP indicates damage-associated molecular pattern; HMGB1, high mobility group box-1; IL, interleukin; PBS, phosphate-buffered saline; PCR, polymerase chain reaction.

than that observed with the sham procedure alone. Of note, the degree of myocardial inflammation was not significantly different (P=0.88) between saline injection and injection of denatured NMC supernatants. However, the remarkable finding shown by Figure 13 is that injection of NMC supernatants provoked a robust inflammatory response that was significantly (P=0.005 for both) greater than that obtained with injection of saline or denatured NMC-injected hearts. We also examined collagen volume in the same hearts. The group data in Figure 13D demonstrate that picrosirius red staining was significantly (P=0.004 and 0.005, respectively) greater in the hearts injected with NMCs, compared with either saline-injected or denatured NMCs. To determine whether the observed cardiac extract-induced myocardial inflammation and fibrosis was mediated through TLR4 signaling, as suggested by our in vitro studies, we also injected NMC supernatants into the LV apex of TLR4-deficient mice and their respective littermate controls. As shown by the representative data in Figure 13A and 13C and the group data illustrated in Figure 13B and 13D, there was no significant difference in the extent of myocardial inflammation (P=0.22) or myocardial fibrosis (P=0.20) in the NMC-injected TLR4 knockout mice, compared with denatured NMC-treated wild-type mice with intact TLR4 signaling.

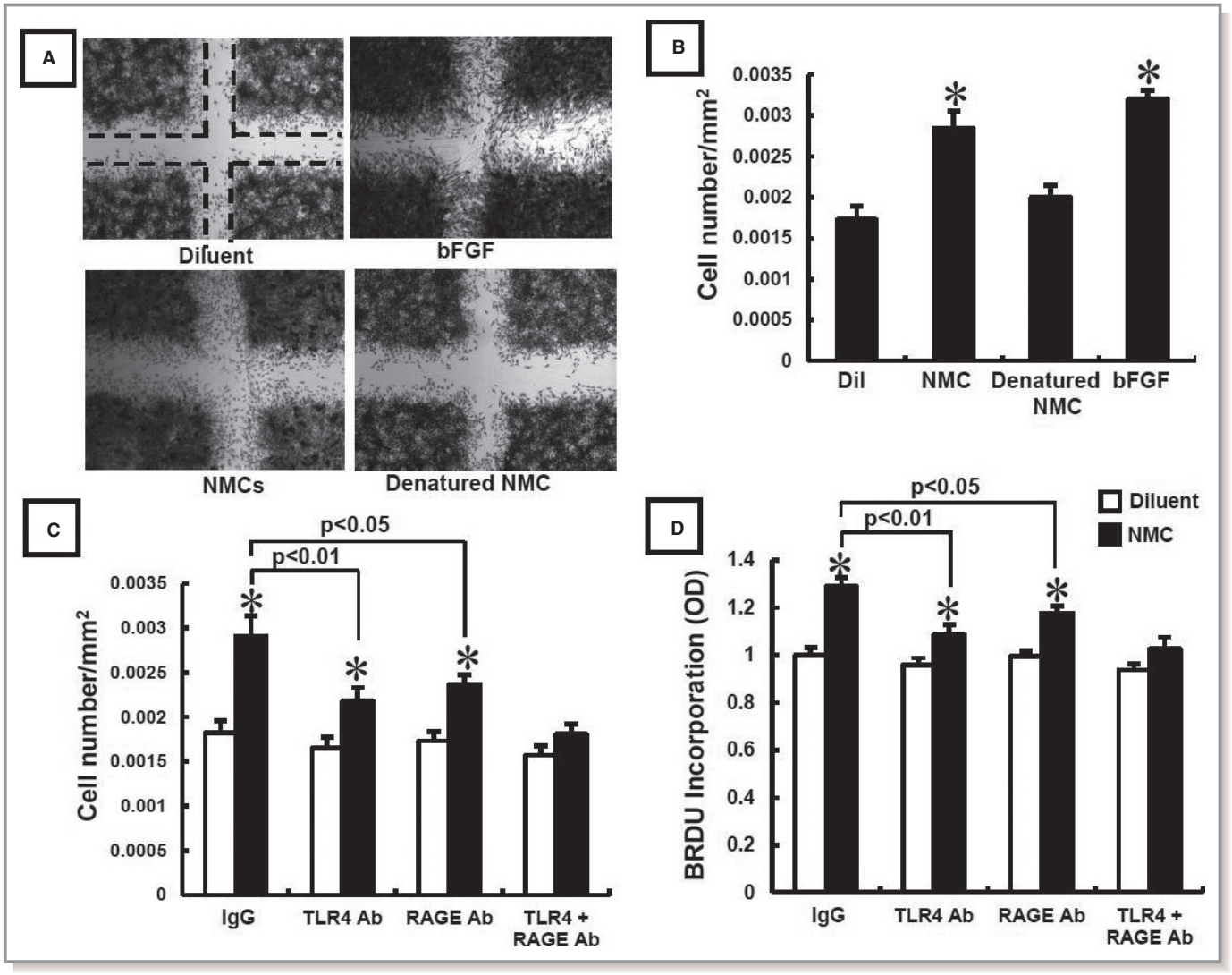

Figure 8. Effect of NMC supernatants on fibroblast migration. A, Representative phase-contrast micrographs (×50) of scratched cell NIH/3T3 fibroblast monolayers stimulated for 36 hours with diluent (PBS), NMC supernatants, denatured NMC supernatants, or bFGF (positive control). The number of cells migrating into the "region of interest" represented by the orthogonal dotted lines illustrated in the PBS-treated fibroblasts by the lines was used to enumerate the number of migrating cells. B, Results of group data for fibroblasts treated for 36 hours with PBS, NMC supernatants (10 μg/mL), denatured NMC supernatants (10 μg/mL), and bFGF (25 ng/mL). C, Results of group data for fibroblasts treated with diluent or NMC supernatants (10 μg/mL), in the presence of IgG, TLR4 antibody (Ab), RAGE Ab, and TLR4 Ab+RAGE Ab (n=9 dishes for each experimental group from 3 independent experiments). D, Group data for BrdU incorporation in NIH/3T3 fibroblasts stimulated with diluent or 10 μg/mL NMC supernatants for 72 hours in the presence and absence of IgG, TLR4 Ab, RAGE, and TLR4 Ab+RAGE Ab (n=6 for each group from 3 independent experiments) (*P<0.05 compared with diluent). bFGF indicates basic fibroblast growth factor; BrdU, bromodeoxyuridine (5-bromo-2′-deoxyuridine); NMC, necrotic myocardial cell; PBS, phosphate-buffered saline; RAGE, receptor for advance glycation end products; TLR4, Toll-like receptor-4.

Mechanism for the Effects of NMC Supernatants

Immunodepletion

To elucidate the mechanism for the effects of the NMC supernatants on fibroblast proliferation, the NMC supernatants were treated with a neutralizing HMGB1 (10 μg/mL) antibody. As shown in Figure 14A, treatment with an HMGB1 neutralizing antibody abrogated the proliferative effects of 0.1 μg/mL recombinant HMGB1 (P=0.06 compared with diluent), as well the proliferative effects of NMC (P=0.06 compared with diluent) supernatants (10 μg/mL). Importantly, neither treatment with an equimolar concentration of an isotype IgG control antibody nor treatment with a neutralizing HMGB1 (10 μg/mL) antibody had any effect (P=0.37) on NMC-induced fibroblast proliferation.

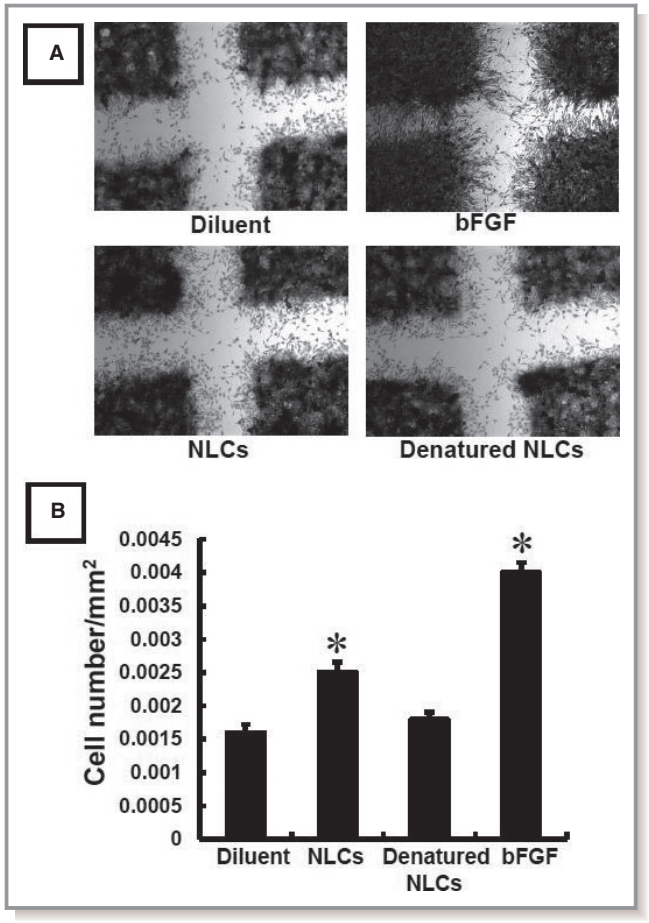

Figure 9. Effects of necrotic liver cells on NIH/3T3 fibroblast cell migration. A, Representative phase-contrast micrographs (×50) of scratched cell monolayers stimulated for 36 hours with diluent (PBS), NLCs, D-NLCs, or bFGF (positive control). B, Results of group data for fibroblasts treated for 36 hours with PBS (NLCs; 10 μg/mL), D-NLCs (10 μg/mL), and bFGF (25 ng/mL) (*P<0.05 compared with PBS). bFGF indicates basic fibroblast growth factor; D-NLC, denatured necrotic liver cell; NLC, necrotic liver cell; PBS, phosphate-buffered saline.

Effect of HMGB1 in vivo

To determine whether HMGB1 was sufficient to provoke myocardial inflammation and fibrosis in vivo, we injected recombinant HMGB1 into the LV apex of wild-type C57/Bl6 and TLR4-deficient mouse hearts and examined myocardial inflammation and myocardial fibrosis at 72 hours. Figure 14B depicts representative histological myocardial sections from hearts that were injected with denatured HMGB1 and recombinant HMGB1; group data are summarized in Figure 14C. Injection of recombinant HMGB1in wild-type hearts provoked a robust inflammatory response that was significantly greater than that observed with denatured HMGB1 (P=0.009). Remarkably, the extent of myocardial inflammation in HMGB1-injected TLR4$^{-/-}$ mouse hearts was not significantly different (P=0.52) than that observed in wild-type mouse hearts that were injected with denatured HMGB1. We also examined collagen volume in the same hearts. As shown by the representative images in Figure 14D and the group data in Figure 14E, the extent of picrosirius red staining was significantly greater (P=0.005) in the wild-type mouse hearts that were injected with HMGB1 compared with wild-type hearts injected with denatured HMGB1. However, the effects of HMGB1 on myocardial fibrosis were not significantly different (P=0.54) in TLR4$^{-/-}$ mouse hearts, compared with wild-type mouse hearts injected with denatured HMGB1 Viewed together, the in vitro and in vivo studies suggest that HMGB1 is an essential mediator of NMC-induced myocardial inflammation and myocardial fibrosis.

Discussion

The ability of the myocardium to successfully compensate for and adapt to environmental stress ultimately determines whether the heart will decompensate and fail or whether it will instead maintain preserved function. Despite the importance of the myocardial response to environmental stress, very little is known with respect to the basic mechanisms that are responsible for initiating stress responses in the heart. Here, we show for the first time that proteins released by NMCs are sufficient to initiate a repertoire of repair mechanisms in fibroblasts through activation of TLR4, a canonical innate immune PRR. Three distinct but mutually complementary scientific lines of evidence support this conclusion. First, Western blot analysis of supernatants from NMCs revealed the presence of several classic DAMPs, including HGMB1, galectin-3, S100β, S100A8, S100A9, and IL-1α (Figure 2A). Treatment of fibroblasts with supernatants from NMCs increased fibroblast proliferation (Figure 2B and 2D), fibroblast α-SMA activation (Figure 4A and 4B), fibroblast expression levels of collagen 1A1 and collagen 3A1 (Figure 4C), and fibroblast migration (Figure 8B). The effects of NMC supernatants on fibroblast proliferation were sensitive to heat denaturation but were unaffected by treatment with DNase or RNase, suggesting that the stimulatory molecules present in the NMC supernatants were proteins and not nucleic acids. In a cell-wounding assay, NMC supernatants induced increased fibroblast migration into the denuded area, which could be partially inhibited by using a TLR4 or RAGE antibody and completely inhibited by simultaneous treatment with TLR4 and RAGE antibodies or by heat denaturing the NMC supernatants (Figure 8B and 8C). Noting that both Akt and MAPKs were downstream from TLR- and RAGE-dependent signaling, we measured Akt and MAPK activity levels in diluent and NMC-treated fibroblast cultures. NMC supernatants increased Akt and Erk phosphorylation in cultured fibroblasts in a time-dependent manner, whereas inhibition of Akt and

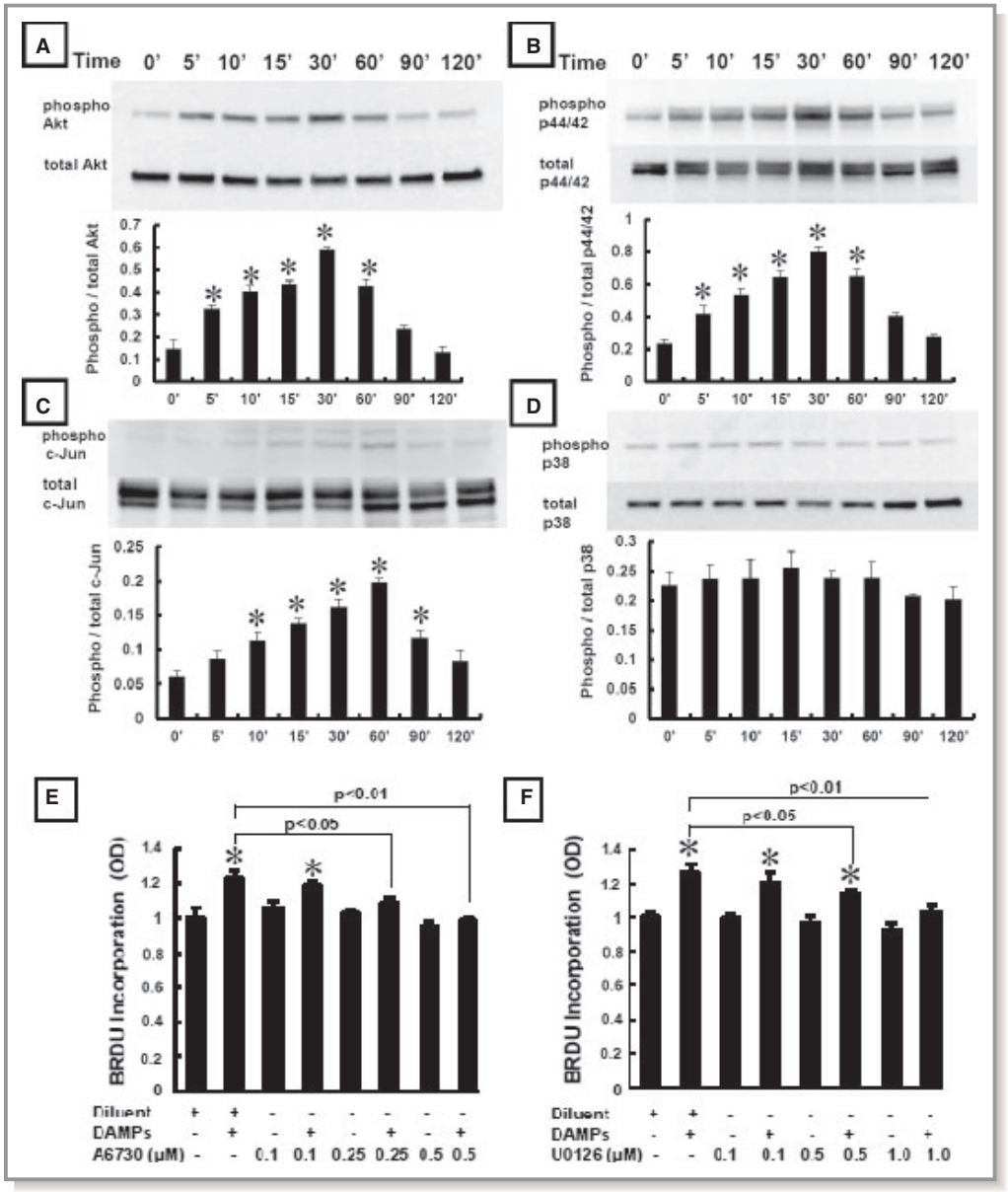

Figure 10. Effect of NMCs on MAPK and signaling in fibroblasts. NIH/3T3 fibroblast cultures were stimulated with NMC (10 μg/mL) supernatants for the times indicated to determine Akt (A), ERK (p44/42) (B), c-Jun (C), and p38 (D) activity. Representative Western blots for phospho- Akt, ERK, c-Jun, and p-38 and total-Akt, ERK, c-Jun, and p-38 are illustrated in the upper panels and group data (expressed as the ratio of the intensity of the bands corresponding to phosphorylated/total protein) are shown in the lower panels. All experiments were performed in triplicate (**P*<0.05 compared with baseline [0 minutes]). E, Effect of pretreatment (30 min) with 0.1, 0.25, and 0.5 μmol/L A6730 (Akt inhibitor) on NMC-induced BrdU incorporation in fibroblasts. F, Effect of pretreatment (30 min) with 0.1, 0.5, and 1.0 μmol/L U0126 (ERK inhibitor) on NMC-induced BrdU incorporation in fibroblasts (n=6 dishes for each experimental group taken from 3 independent experiments) (**P*<0.05 compared with diluent). All experiments were performed in triplicate. BrdU indicates bromodeoxyuridine (5-bromo-2′-deoxyuridine); DAMP, damage-associated molecular pattern; MAPK, mitogen activated protein kinase; NMC, necrotic myocardial cell; OD, optical density.

Erk signaling with specific inhibitors (A6730 and U0126, respectively) abolished fibroblast proliferation in a concentration manner (Figure 10). Remarkably, similar responses in terms of fibroblast proliferation and motility were observed with supernatants obtained from NLCs (Figures 3 and 9), suggesting that the biologically active properties of necrotic cells were not unique to cell types residing in the heart. Second, the effects of NMC supernatants on fibroblast

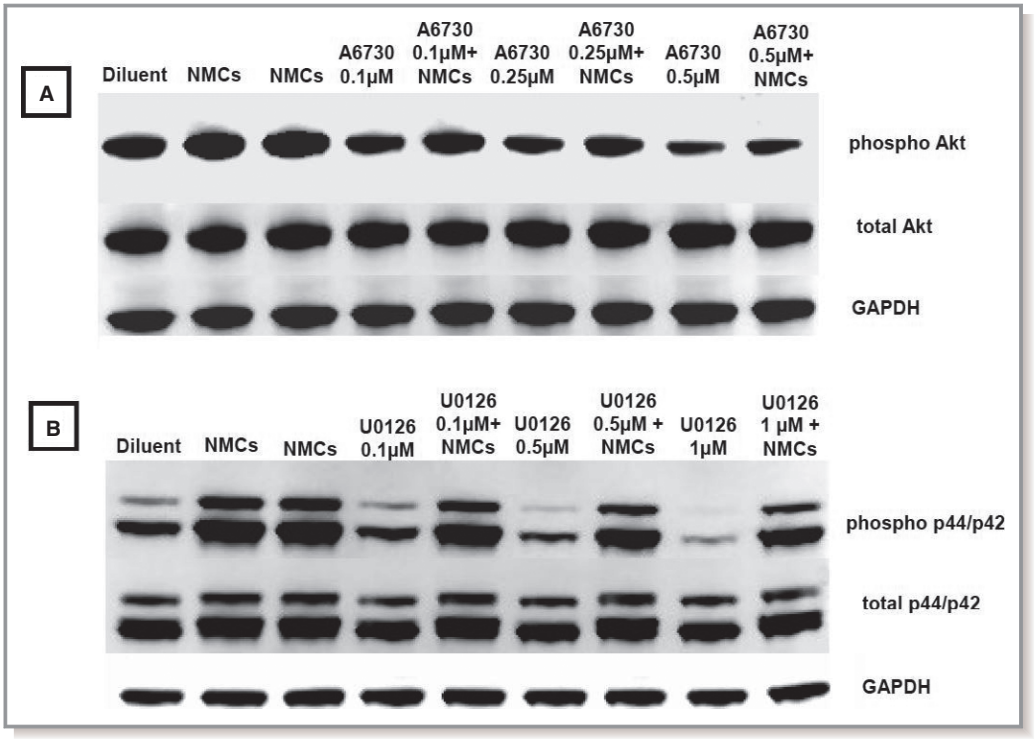

Figure 11. Effect of A6730 on Akt phosphorylation and U0126 on Erk activity. A, Representative Western blot of phospho-Akt and total Akt levels in NIH/3T3 cells (see text for details). Fibroblast cultures were pretreated (30 minutes) with 0.1, 0.25, and 0.5 μmol/L A6730 or diluent and then stimulated for 30 minutes with necrotic myocardial cell (NMC) supernatants (10 μg/mL). B, Representative Western blot of phospho-Erk and total Erk levels in NIH/3T3 cells pretreated (30 minutes) with 0.1, 0.5, and 1.0 μmol/L U0126 or diluent (same volume of DMSO) and then stimulated for 30 minutes with NMC supernatants (10 μg/mL). All experiments were performed in triplicate.

proliferation were mimicked, in a concentration-dependent manner, by several purified recombinant DAMPs that were immunodetectable in the NMC supernatants, including HMGB1, galectin-3, and S100A8/S100A9 (Figure 5), whereas only HMGB1 and galectin-3 increased collagen 1A1 and collagen 3A1 gene expression (Figure 7). Treatment of fibroblasts with multiple recombinant DAMPs that were biologically inactive at lower concentrations increased fibroblast proliferation to the same extent as did NMC supernatants (Figure 6), suggesting that low concentrations of DAMPs can act synergistically to induce fibroblast proliferation. Third, injection of NMC supernatants induced inflammation and myocardial fibrosis in vivo (Figure 13). Importantly, the extent of inflammation and myocardial fibrosis after the injection of thermally denatured NMCs was not different than that observed with needle injury alone (Figure 13). Consistent with our in vitro observations, the effects of NMC supernatants on myocardial inflammation and myocardial fibrosis were absent in TLR4-deficient mice (Figure 13). Although these studies were not intended to identify the biological effects of the entire portfolio of DAMPs released by NMCs, under the simple well-defined experimental conditions used in this study, we show that HMGB1 is necessary and sufficient for fibroblast activation in vivo (Figure 14A and 14B) as well as in vitro (Figures 5 and 7). Further, injection of HMBG1 into wild-type hearts provoked myocardial inflammation and fibrosis in vivo, whereas the proinflammatory effects of HMGB1 in vivo were abrogated by heat denaturation and were not detectable in the hearts of TLR4-deficient mice (Figure 14). Viewed together, these data constitute the initial demonstration that proteins released by NMCs are sufficient to induce fibroblast activation, myocardial inflammation, and myocardial fibrosis, through activation of classic innate immune signaling pathways.

Tissue Injury and DAMPs

The biological activity of DAMPs is exceedingly complex and depends on a variety of factors, including the overall extent of tissue injury, the type of cell death (necrosis versus apoptosis), and the type of cells dying (epithelial versus mesenchymal). DAMPs can be subdivided into 3 broad categories: (1) intracellular molecules released by dying cells (S100 proteins, HMGB1, IL-1α, galectin-3, heat shock protein [HSP]

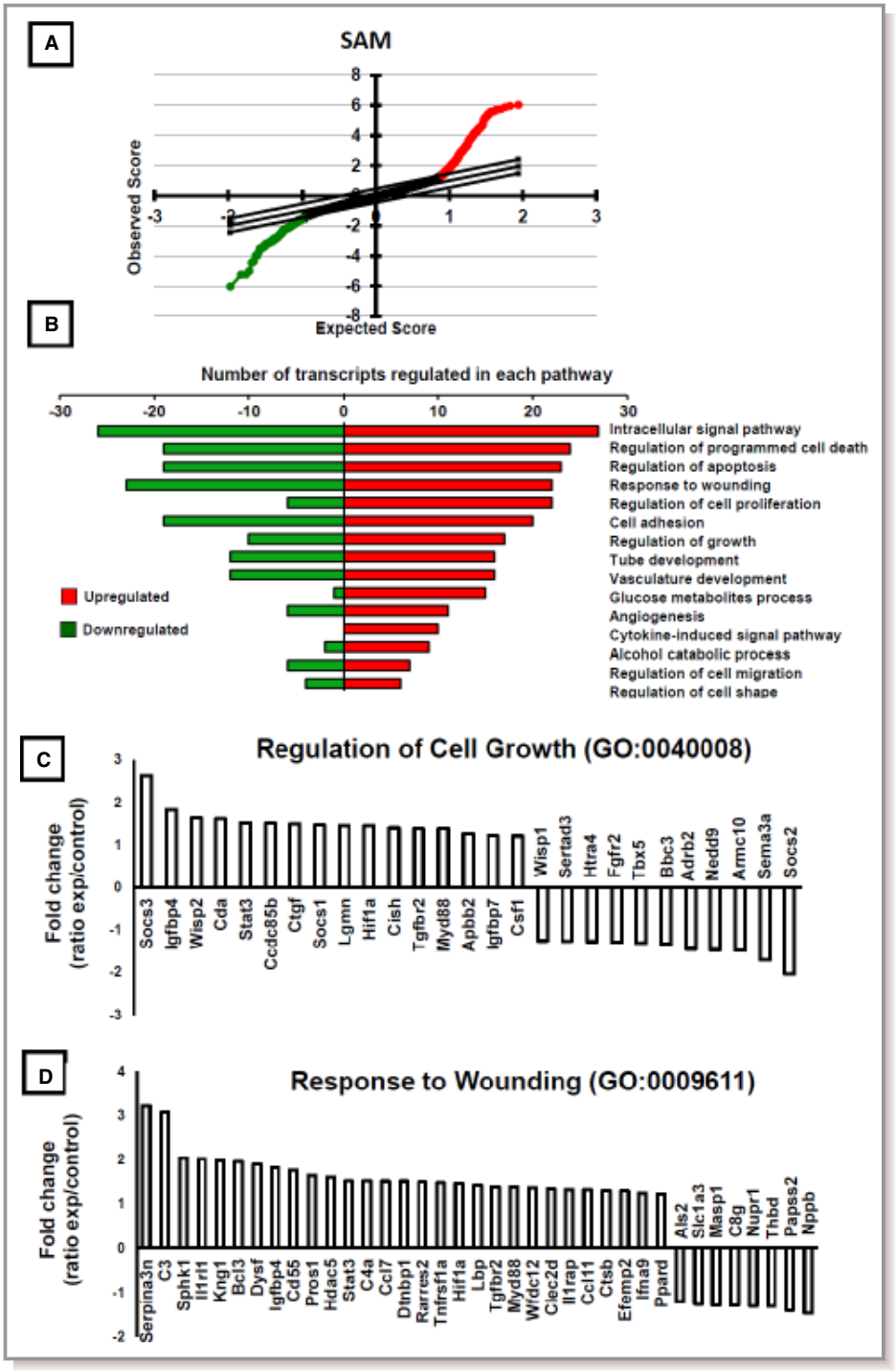

Figure 12. Transcriptional profiling in NMC-stimulated fibroblasts. A, SAM plot of changes in gene expression in NIH/3T3 fibroblasts stimulated with 10 μg/mL NMC supernatants compared with diluent-treated controls (n=4 separate cultures/group). Genes that were significantly increased are denoted by red circles; genes that were significantly decreased are denoted by green circles. An FDR <5% was used for the SAM plots. B, GO analysis of functional pathways that were significantly different in the NMC-stimulated fibroblast cultures compared with diluent. C and D, GO analysis of significant changes in gene expression in NMC supernatant (10 μg/mL) stimulated NIH/3T3 fibroblasts (relative to diluent). C, Significant changes in gene expression (fold-change) in the cell growth pathway (GO:0040008). D, Significant changes in gene expression (fold-change) in the response to wounding pathway (GO:0009611) (n=4 samples/group). FDR indicates false discovery rate; GO, gene ontology; NMC, necrotic myocardial cell; SAM, Statistical Analysis of Microarray.

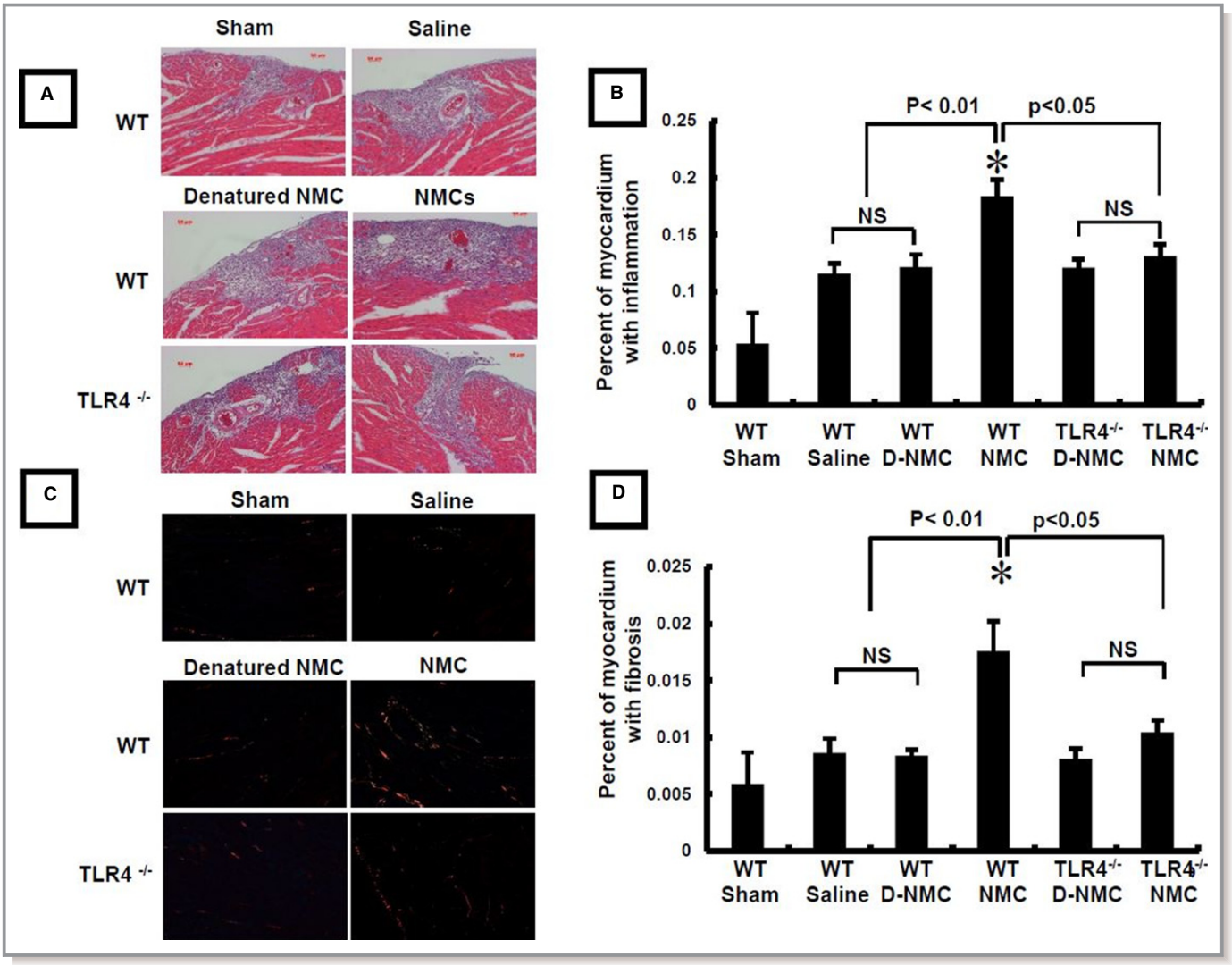

Figure 13. Effect of NMC supernatants on myocardial inflammation and myocardial fibrosis. A, Representative histological myocardial sections of myocardial inflammation from WT and TLR4-deficient ($TLR4^{-/-}$) mice that were sham-operated or injected with saline, D-NMC supernatants, or NMC supernatants (×50 magnification). B, Group data for myocardial inflammation (expressed as percentage of myocardial area) for WT and TLR4-deficient mice that were sham-operated mice or injected with saline, D-NMC supernatants, or NMC supernatants (n=5 or 6 hearts/group). C, Representative picrosirius red staining of myocardial sections (×100 magnification) from WT or TLR4-deficient mice. D, Group data for picrosirius red staining (expressed as percentage of myocardial area) for WT and TLR4-deficient mice that were sham-operated mice or injected with saline, D-NMC supernatants, or NMC supernatants (n=5 or 6 hearts/group) (*P<0.05 compared with sham operated controls). D-NMC indicates denatured necrotic myocardial cell; NMC, necrotic myocardial cell; TLR4, Toll-like receptor-4; WT, wild-type.

60, HSP 70, HSP 72[22]) and/or molecules that are expressed on the cell surface membranes of stressed of dying cells (eg, phosphatidylserine), (2) leaderless proteins secreted by professional immune cells, also referred to as "alarmins" (eg, HMGB1, IL-1β, galectin-3, uric acid), and (3) components of the extracellular matrix (hyaluronan, heparan sulfate, fibronectin, and degraded matrix constituents). The precise biochemical moieties that distinguish whether an intracellular protein is immunogenic or nonimmunogenic are unclear; however, it has been proposed that many known DAMPs, such as the chaperones belonging to the HSP family, contain hydrophobic regions that are ordinarily hidden in healthy living cells and become immunogenic when released into the extracellular space.[23] Furthermore, studies have shown the proinflammatory properties of DAMPs such as HMGB1 and S100A8/S100A9 are highly sensitive to the redox microenvironment in the extracellular space. The extracellular milieu in healthy tissues is oxidizing, which leads to the denaturation and inactivation of DAMPs that are released into the extracellular space. In contrast, the release of oxidoreductases and nonthiol proteins in injured tissue modifies the extracellular redox state to a reducing environment, which can increase the proinflammatory properties of DAMPs.[24,25] For example, the *S*-thiolation status of cysteine residues 23, 45,

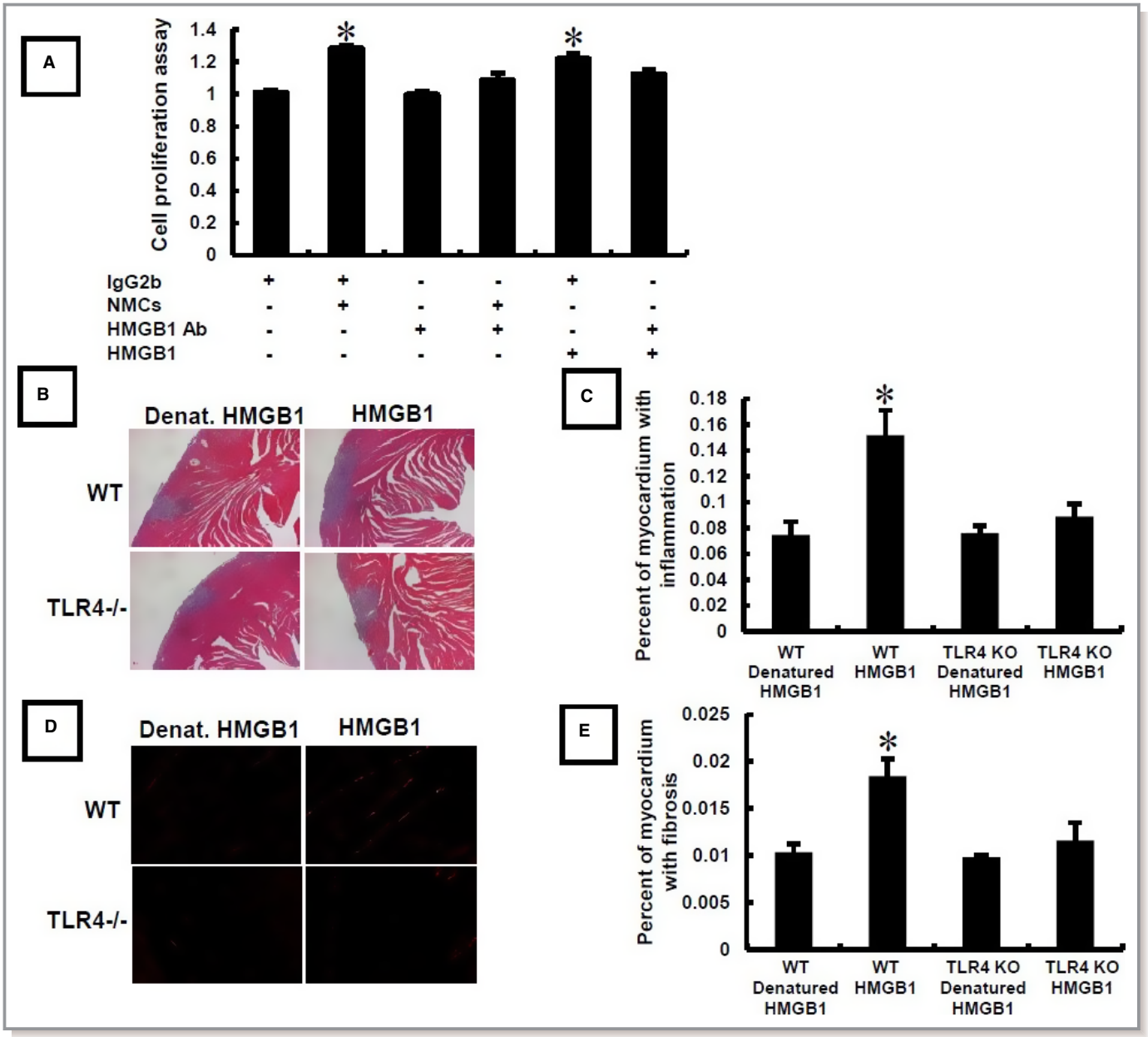

Figure 14. Effects of HMGB1 in vitro and in vivo. A, BrdU incorporation in NIH/3T3 fibroblasts stimulated with NMC (10 μg/mL) supernatants or recombinant HMGB1, in the presence and absence of IgG2b or an HMGB1 antibody (n=4 to 6 dishes from 3 separate experiments) (**P*<0.05 compared with IgG2b control antibody alone). B, Representative myocardial sections (×50 magnification) of myocardial inflammation from WT and TLR4-deficient ($TLR4^{-/-}$) mice that were injected with 200 ng/10 μL HMGB1 or 200 ng/10 μL denatured HMGB1. C, Group data for myocardial inflammation (expressed as percentage of myocardial area) for WT and TLR4-deficient mice injected with 200 ng/10 μL HMGB1 or 200 ng/10 μL denatured HMGB1. D, Representative picrosirius red staining of myocardial sections (×100 magnification) from WT and TLR4-deficient mice that were injected with 200 ng/10 μL HMGB1 or 200 ng/10 μL denatured HMGB1 (×100 magnification). E, Group data for picrosirius red staining (expressed as percentage of myocardial area) in WT and TLR4-deficient mice that were injected with 200 ng/10 μL HMGB1 or 200 ng/10 μL denatured HMGB1 (n=5 or 6 hearts/group) (**P*<0.05 compared with WT mice treated with denatured HMGB1). BrdU indicates bromodeoxyuridine (5-bromo-2′-deoxyuridine); HMGB1, high mobility group box-1; KO, knock-out; NMC, necrotic myocardial cell; TLR4, Toll-like receptor-4; WT, wild-type.

and 106 on HMGB1 determines whether this chromatin binding protein engages TLRs and acts as a proinflammatory cytokine or whether it is biologically inert when released into the extracellular space.[25] Additional complexity of DAMP signaling is conferred by the formation of heterocomplexes with other immune coactivators such as C-X-C motif chemokine 12, lipolysaccharide, or IL-1β, which may generate synergistic responses in inflammation.[26]

While these comments have focused on the proinflammatory effects of DAMPs, it bears emphasis that DAMP-induced inflammation is essential to restore tissue homeostasis by activating tissue repair mechanisms in vivo. DAMPs activate macrophages, dendritic cells, and endogenous precursor stem cells that are required for initiating tissue repair.[8,27,28] DAMPs have been shown to induce the proliferation of smooth muscle cells and fibroblasts[29] and to stimulate angiogenesis[30] and skeletal and cardiac myogenesis,[27,30] as well as to promote regeneration of renal tubule cells and liver cells.[31,32] These reports are consistent with the observations in the present study, wherein we demonstrate that cardiac DAMPs are sufficient to increase fibroblast proliferation and mobility, increase collagen synthesis, and activate a repertoire of gene ontologies that are involved in the response to wounding and angiogenesis (Figure 12). We further show that HMGB1, a nonhistone nuclear protein that has been referred to as the "master regulator of innate immunity,"[28] has a nonredundant role with respect to fibroblast activation in vitro. Relevant to the present discussion, HMGB1 is capable of eliciting pleiotropic effects that depend on its cellular location, context, and posttranslational modification.[33] In response to myocardial injury, HMGB1 translocates from the nucleus to the cytoplasm in cardiac myocytes and can be released into the extracellular space through nonclassic secretory mechanisms.[34,35] The pleiotropic effects of HMGB1 are in part related to the plasticity of HMGB1–receptor interactions, when HMGB1 forms complexes with selected ligands (eg, IL-1α/β), signaling proteins (eg, CD24 and Siglec-10), and/or DNA, RNA, and histone proteins.[33] Not surprisingly, both beneficial and deleterious roles have been proposed for HMGB1 in different models of cardiac injury, which likely reflects the complex and context-dependent biology of HMGB1.[2,22] Because the NIH-3T3 cells used herein were relatively less sensitive to the effects of DAMPs than primary cardiac fibroblasts, we cannot exclude the possibility that the effects of DAMPs on fibroblast activation and/or gene expression may have been more robust than we observed.

Conclusions

The results of the present study provide an important and previously undefined mechanistic link between necrotic cell death, activation of innate immune signaling, and the onset of tissue repair in the heart. Although the release of DAMPs by NMCs is likely essential for beneficial healing responses in the heart, sustained DAMP signaling may also lead to excessive inflammation and adverse LV remodeling because of sustained DAMP-induced inflammation and/or enhanced B- and T-cell responses that arise secondary to processing of DAMPs by mononuclear phagocytes residing in and/or that are recruited to the myocardium after tissue injury.[36,37] Thus, the relative contribution of DAMP-mediated signaling to adaptive and maladaptive responses in the heart will likely be both time and context dependent. These studies raise the intriguing possibility that it may be possible to identify candidate DAMPs that can be exploited as therapeutic targets. As one example, HMGB1-specific antagonists have been shown to be effective in a variety of different animal disease models, including arthritis, stroke, sepsis, and organ transplantation.[33] Moreover, certain motifs residing in DAMPs may be used therapeutically to exploit regenerative cues for resident cardiac progenitor cells and/or infiltrating cells. For example, necrotic cell debris enhances the ability of a collagen-based extracellular matrix to stimulate myogenesis in the *mdx* mouse model of Duchenne muscular dystrophy.[38] Finally, although speculative, it is possible that the release of DAMPs by injected cardiac stem cells may explain, at least in part, the paradox between the lack of engraftment of these cells and their observed "paracrine" effects on tissue repair and angiogenesis.[39] Accordingly, further elucidation of the spatial and temporal role of DAMPs with respect to activating innate and adaptive immune responses in the heart should provide important insights into the role of the immune system in mediating adaptive and maladaptive cardiac remodeling.

Sources of Funding

This research was supported by research funds from the National Institutes of Health (RO1 HL58081, RO1 HL61543, RO1 HL42250, and T32 HL07816).

Disclosures

None.

References

1. Frangogiannis NG. The mechanistic basis of infarct healing. *Antioxid Redox Signal*. 2006;8:1907–1939.
2. Arslan F, de Kleijn DP, Pasterkamp G. Innate immune signaling in cardiac ischemia. *Nat Rev Cardiol*. 2011;8:292–300.
3. Kono H, Rock KL. How dying cells alert the immune system to danger. *Nat Rev Immunol*. 2008;8:279–289.
4. Rock KL, Latz E, Ontiveros F, Kono H. The sterile inflammatory response. *Annu Rev Immunol*. 2010;28:321–342.
5. Matzinger P. Tolerance, danger, and the extended family. *Annu Rev Immunol*. 1994;12:991–1045.
6. Janeway CA Jr. Approaching the asymptote? Evolution and revolution in immunology. *Cold Spring Harb Symp Quant Biol*. 1989;54(Pt 1):1–13.
7. Janeway CA Jr, Medzhitov R. Introduction: the role of innate immunity in the adaptive immune response. *Semin Immunol*. 1998;10:349–350.
8. Takeuchi O, Akira S. Pattern recognition receptors and inflammation. *Cell*. 2010;140:805–820.
9. Zhang W, Chancey AL, Tzeng HP, Zhou Z, Lavine KJ, Gao F, Sivasubramanian N, Barger PM, Mann DL. The development of myocardial fibrosis in transgenic mice with targeted overexpression of tumor necrosis factor requires mast cell-fibroblast interactions. *Circulation*. 2011;124:2116.

10. Takeuchi O, Hoshino K, Kawai T, Sanjo H, Takada H, Ogawa T, Takeda K, Akira S. Differential roles of TLR2 and TLR4 in recognition of gram-negative and gram-positive bacterial cell wall components. *Immunity*. 1999;11:443–451.
11. Scaffidi P, Misteli T, Bianchi ME. Release of chromatin protein HMGB1 by necrotic cells triggers inflammation. *Nature*. 2002;418:191–195.
12. Ranzato E, Patrone M, Pedrazzi M, Burlando B. Hmgb1 promotes wound healing of 3T3 mouse fibroblasts via RAGE-dependent ERK1/2 activation. *Cell Biochem Biophys*. 2010;57:9–17.
13. Mitola S, Belleri M, Urbinati C, Coltrini D, Sparatore B, Pedrazzi M, Melloni E, Presta M. Cutting edge: extracellular high mobility group box-1 protein is a proangiogenic cytokine. *J Immunol*. 2006;176:12–15.
14. Tekabe Y, Li Q, Rosario R, Sedlar M, Majewski S, Hudson BI, Einstein AJ, Schmidt AM, Johnson LL. Development of receptor for advanced glycation end products-directed imaging of atherosclerotic plaque in a murine model of spontaneous atherosclerosis. *Circ Cardiovasc Imaging*. 2008;1:212–219.
15. Divakaran VG, Evans S, Topkara VK, Diwan A, Burchfield J, Gao F, Dong J, Tzeng HP, Sivasubramanian N, Barger PM, Mann DL. Tumor necrosis factor receptor associated factor 2 signaling provokes adverse cardiac remodeling in the adult mammalian heart. *Circ Heart Fail*. 2013;6:535–543.
16. Yang L, Seki E. Toll-like receptors in liver fibrosis: cellular crosstalk and mechanisms. *Front Physiol*. 2012;3:138.
17. Anders HJ, Schaefer L. Beyond tissue injury-damage-associated molecular patterns, toll-like receptors, and inflammasomes also drive regeneration and fibrosis. *J Am Soc Nephrol*. 2014;25:1387–1400.
18. Bechtel W, McGoohan S, Zeisberg EM, Muller GA, Kalbacher H, Salant DJ, Muller CA, Kalluri R, Zeisberg M. Methylation determines fibroblast activation and fibrogenesis in the kidney. *Nat Med*. 2010;16:544–550.
19. Yang J, Chen L, Yang J, Ding J, Rong H, Dong W, Li X. High mobility group box-1 induces migration of vascular smooth muscle cells via TLR4-dependent PI3K/Akt pathway activation. *Mol Biol Rep*. 2012;39:3361–3367.
20. Palumbo R, Sampaolesi M, De MF, Tonlorenzi R, Colombetti S, Mondino A, Cossu G, Bianchi ME. Extracellular HMGB1, a signal of tissue damage, induces mesoangioblast migration and proliferation. *J Cell Biol*. 2004;164:441–449.
21. Bonaldi T, Talamo F, Scaffidi P, Ferrera D, Porto A, Bachi A, Rubartelli A, Agresti A, Bianchi ME. Monocytic cells hyperacetylate chromatin protein HMGB1 to redirect it towards secretion. *EMBO J*. 2003;22:5551–5560.
22. Lin L, Knowlton AA. Innate immunity and cardiomyocytes in ischemic heart disease. *Life Sci*. 2014;100:1–8.
23. Seong SY, Matzinger P. Hydrophobicity: an ancient damage-associated molecular pattern that initiates innate immune responses. *Nat Rev Immunol*. 2004;4:469–478.
24. Lim SY, Raftery MJ, Geczy CL. Oxidative modifications of DAMPs suppress inflammation: the case for S100A8 and S100A9. *Antioxid Redox Signal*. 2011;15:2235–2248.
25. Yang H, Lundback P, Ottosson L, Erlandsson-Harris H, Venereau E, Bianchi ME, Al-Abed Y, Andersson U, Tracey KJ, Antoine DJ. Redox modification of cysteine residues regulates the cytokine activity of high mobility group box-1 (HMGB1). *Mol Med*. 2012;18:250–259.
26. Chen R, Hou W, Zhang Q, Kang R, Fan XG, Tang D. Emerging role of high-mobility group box 1 (HMGB1) in liver diseases. *Mol Med*. 2013;19:357–366.
27. Limana F, Germani A, Zacheo A, Kajstura J, Di Carlo A, Borsellino G, Leoni O, Palumbo R, Battistini L, Rastaldo R, Muller S, Pompilio G, Anversa P, Bianchi ME, Capogrossi MC. Exogenous high-mobility group box 1 protein induces myocardial regeneration after infarction via enhanced cardiac C-kit+ cell proliferation and differentiation. *Circ Res*. 2005;97:e73–e83.
28. Vezzoli M, Castellani P, Corna G, Castiglioni A, Bosurgi L, Monno A, Brunelli S, Manfredi AA, Rubartelli A, Rovere-Querini P. High-mobility group box 1 release and redox regulation accompany regeneration and remodeling of skeletal muscle. *Antioxid Redox Signal*. 2011;15:2161–2174.
29. Kuraitis D, Ebadi D, Zhang P, Rizzuto E, Vulesevic B, Padavan DT, Al MA, McEwan KA, Sofrenovic T, Nicholson K, Whitman SC, Mesana TG, Skerjanc IS, Musaro A, Ruel M, Suuronen EJ. Injected matrix stimulates myogenesis and regeneration of mouse skeletal muscle after ischaemic injury. *Eur Cell Mater*. 2012;24:175–195.
30. De Mori R, Straino S, Di CA, Mangoni A, Pompilio G, Palumbo R, Bianchi ME, Capogrossi MC, Germani A. Multiple effects of high mobility group box protein 1 in skeletal muscle regeneration. *Arterioscler Thromb Vasc Biol*. 2007;27:2377–2383.
31. Romagnani P, Anders HJ. What can tubular progenitor cultures teach us about kidney regeneration? *Kidney Int*. 2013;83:351–353.
32. Yang R, Zhang S, Cotoia A, Oksala N, Zhu S, Tenhunen J. High mobility group B1 impairs hepatocyte regeneration in acetaminophen hepatotoxicity. *BMC Gastroenterol*. 2012;12:45.
33. Harris HE, Andersson U, Pisetsky DS. HMGB1: a multifunctional alarmin driving autoimmune and inflammatory disease. *Nat Rev Rheumatol*. 2012;8:195–202.
34. Sakata Y, Dong JW, Vallejo JG, Huang CH, Baker JS, Tracey KJ, Tacheuchi O, Akira S, Mann DL. Toll-like receptor 2 modulates left ventricular function following ischemia-reperfusion injury. *Am J Physiol Heart Circ Physiol*. 2007;292:H503–H509.
35. Xu H, Su Z, Wu J, Yang M, Penninger JM, Martin CM, Kvietys PR, Rui T. The alarmin cytokine, high mobility group box 1, is produced by viable cardiomyocytes and mediates the lipopolysaccharide-induced myocardial dysfunction via a TLR4/phosphatidylinositol 3-kinase gamma pathway. *J Immunol*. 2010;184:1492–1498.
36. Ismahil MA, Hamid T, Bansal SS, Patel B, Kingery JR, Prabhu SD. Remodeling of the mononuclear phagocyte network underlies chronic inflammation and disease progression in heart failure: critical importance of the cardiosplenic axis. *Circ Res*. 2014;114:266–282.
37. Hofmann U, Beyersdorf N, Weirather J, Podolskaya A, Bauersachs J, Ertl G, Kerkau T, Frantz S. Activation of CD4+ T lymphocytes improves wound healing and survival after experimental myocardial infarction in mice. *Circulation*. 2012;125:1652–1663.
38. Kuraitis D, Berardinelli MG, Suuronen EJ, Musaro A. A necrotic stimulus is required to maximize matrix-mediated myogenesis in mice. *Dis Model Mech*. 2013;6:793–801.
39. Thum T, Bauersachs J, Poole-Wilson PA, Volk HD, Anker SD. The dying stem cell hypothesis: immune modulation as a novel mechanism for progenitor cell therapy in cardiac muscle. *J Am Coll Cardiol*. 2005;46:1799–1802.